Anisotropic Polyconvex Energies on the Basis of Crystallographic Motivated Structural Tensors

J. Schröder[a], P. Neff[b], V. Ebbing[a]

[a]Institut für Mechanik, Fakultät für Ingenieurwissenschaften, Abteilung Bauwissenschaften
Universität Duisburg-Essen, Universitätsstr. 15, 45117 Essen, Germany
[b]Fachbereich Mathematik
Technische Universität Darmstadt, 64289 Darmstadt, Schloßgartenstr. 7, Germany

Abstract

In large strain elasticity the existence of minimizers is guaranteed if the variational functional to be minimized is sequentially weakly lower semicontinuous (s.w.l.s.) and coercive. Therefore, polyconvex functions which are always s.w.l.s. are usually considered. For isotropic as well as for transversely isotropic and orthotropic materials constitutive functions that are polyconvex already exist. The main goal of this contribution is to provide a new method for the construction of polyconvex hyperelastic models for more general anisotropy classes. The fundamental idea is the introduction of positive definite second-order structural tensors $\boldsymbol{G} = \boldsymbol{H}\boldsymbol{H}^T$ encoding the anisotropies of the underlying crystal. These tensors can be viewed as a push-forward of a cartesian metric of a fictitious reference configuration to the real reference configuration. Here the driving transformations $\boldsymbol{H}$ in the push-forward operation are mappings of the cartesian base vectors of the fictitious configuration onto crystallographic motivated base vectors. Restrictions of this approach are based on the polyconvexity condition as well as on the usage of second-order structural tensors and pointed out in detail.

1. State of the Art.

The existence of minimizers is based on the notion of sequential weak lower semicontinuity (s.w.l.s.). If the functional to be minimized is s.w.l.s. and the coercivity condition is fulfilled the existence of minimizers is guaranteed. The concept of quasiconvexity, introduced by MORREY [27], ensures the s.w.l.s. condition if further growth conditions are satisfied. This integral inequality condition implies that the state of minimum energy for a homogeneous body under homogeneous Dirichlet boundary conditions is itself homogeneous. If the stored energy is not quasiconvex, the initially homogeneous material body could break down into coexisting stable phases, see KRAWIETZ [18], BALL & JAMES [4], SILHAVÝ [37], MÜLLER [28], and the references therein. A drawback of the quasiconvexity condition is that the growth condition to be satisfied precludes the physically reasonable requirement $W(\boldsymbol{F}) \to \infty$ for $\det\boldsymbol{F} \to 0^+$, see *problem 1* in BALL [3].

A more attractive notion is, therefore, the polyconvexity condition introduced by BALL [1, 2], because we only have to prove the convexity of the free energy function with respect to the argument $\{\boldsymbol{F}, \mathrm{Cof}\boldsymbol{F}, \det\boldsymbol{F}\} \in \mathbb{R}^{19}$, instead of evaluating the (non-local) integral inequality of the quasiconvexity condition. Considering smooth stored-energy functions the (strict) rank-one convexity implies the (strict) Legendre-Hadamard condition. This is a suitable condition in order to obtain physically reasonable material models, because hereby, the existence of real wave speeds for the corresponding linearization are guaranteed. Instabilities in fiber-reinforced elastic materials induced by loss of ellipticity are discussed in MERODIO & OGDEN [25] and MERODIO & NEFF [24]. For finite-valued, continuous functions we may recapitulate the important implications, that polyconvexity implies quasiconvexity and this implies rank-one convexity; the generalized convexity conditions are depicted in Figure 1. Note that the inverse implications are not true, in this context see also Dacorogna [11], Silhavý [37], Ciarlet [10] and Marsden & Hughes [22].

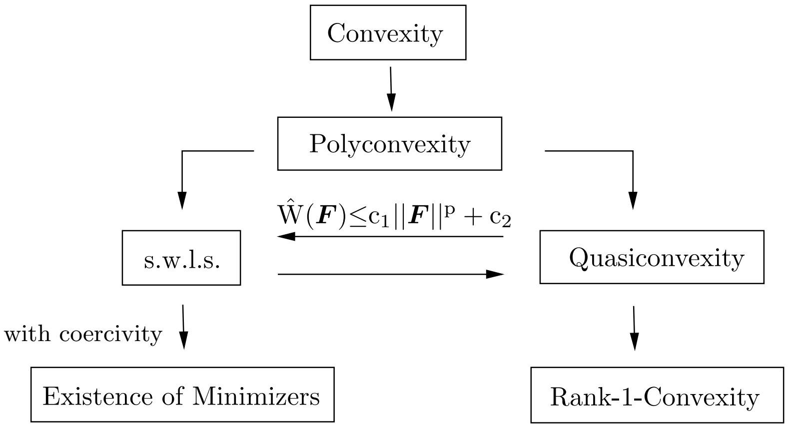

Figure 1: Implication of generalized convexity conditions, s.w.l.s. and existence of minimizers.

For isotropic materials there exist some models, e.g., the Ogden-, Mooney-Rivlin- and Neo-Hooke-type free energy functions, which satisfy the polyconvexity conditions; in this context see also Steigmann [43], Hartmann & Neff [15] and Mielke [26]. In modern applications anisotropic material behavior is often described by isotropic tensor functions. These functions are a result of the isotropicization theorem of anisotropic tensor functions, which states that *an anisotropic constitutive law of a material point, which possesses a physical symmetry group, can be formally expressed as an isotropic function by introducing a set of structural tensors, provided that the set charaterizes the underlying symmetry group of the material.* Here the structural tensors act as additional agencies in the constitutive laws. The concept of structural tensors was first introduced in an attractive way by Boehler [7, 8], see also [9]. Overviews of representations of tensor functions are given in Zhang & Rychlewski [46], Rychlewski & Zhang [31] and Zheng & Spencer [48]. An unified approach summarizing the developments in this field of research can be found in the outstanding review of Zheng [47]. Anisotropic polyconvex energies, especially for the case of transverse isotropy and orthotropy, have been first proposed in Schröder & Neff [32, 33]. Modifications and case studies in the framework presented in [33] are documented in Schröder, Neff & Balzani [34], Balzani [5], Itskov & Aksel [16] and Markert, Ehlers & Karajan [21]. An adjustment of an anisotropic polyconvex model for the simulation of arterial walls to experimental data is given in Balzani et al. [6]. A direct extension of [33] to materials with cubic symmetry is proposed in Kambouchev, Fernandez & Radovitzky [17]. Here the authors introduced a single fourth-order structural tensor that characterizes the associated symmetry group, see [48].

2. Mechanical and Mathematical Preliminaries.

The body of interest in the reference configuration is denoted by $\mathcal{B}_0 \subset \mathbb{R}^3$, parametrized by $\boldsymbol{X}$, and the current configuration by $\mathcal{B}_t \subset \mathbb{R}^3$, parametrized by $\boldsymbol{x}$. The nonlinear deformation map $\boldsymbol{\varphi}_t : \mathcal{B}_0 \mapsto \mathcal{B}_t$ at time $t \in \mathbb{R}_+$ maps points $\boldsymbol{X} \in \mathcal{B}_0$ onto points $\boldsymbol{x} \in \mathcal{B}_t$.

The deformation gradient $\boldsymbol{F}$ is defined by

$$\boldsymbol{F}(\boldsymbol{X}) := \mathrm{Grad}\boldsymbol{\varphi}_t(\boldsymbol{X})\,, \tag{2.1}$$

with the Jacobian $J(\boldsymbol{X}) := \det \boldsymbol{F}(\boldsymbol{X}) > 0$. For the geometrical interpretations of some polynomial invariants we often use expressions based on the mappings of the infinitesimal line $d\boldsymbol{X}$, area $d\boldsymbol{A} = \boldsymbol{N} dA$ and volume elements dV, respectively. These material quantities are mapped to their spatial counterparts $d\boldsymbol{x}$, $d\boldsymbol{a} = \boldsymbol{n} da$ and dv via

$$d\boldsymbol{x} = \boldsymbol{F} d\boldsymbol{X}, \quad \boldsymbol{n} da = \mathrm{Cof}[\boldsymbol{F}]\boldsymbol{N} dA \quad \text{and} \quad dv = \det[\boldsymbol{F}]\, dV\,. \tag{2.2}$$

Equation $(2.2)_2$ is the well-known Nanson's formula. It should already be mentioned that the argument $(\boldsymbol{F}, \mathrm{Cof}\boldsymbol{F}, \det\boldsymbol{F})$ plays an important role in the definition of polyconvexity.

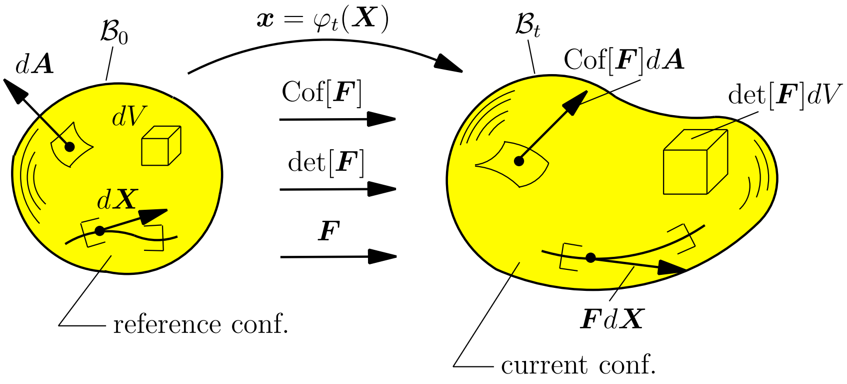

Figure 2: Reference- and actual configuration of the considered body.

For the solution of boundary value problems in finite elasticity we assume the existence of a free energy function $W(\boldsymbol{F})$. The underlying boundary value problem is governed by the variational principle of the potential energy of the whole system with respect to $\boldsymbol{\varphi}$, i.e.,

$$\begin{aligned} \Pi(\boldsymbol{\varphi}) &= \int\limits_{\mathcal{B}_0} W(\boldsymbol{F})\, dV - \int\limits_{\mathcal{B}_0} \rho_0\, \bar{\boldsymbol{b}} \cdot \boldsymbol{\varphi}\, dV - \int\limits_{\partial\mathcal{B}_0} \bar{\boldsymbol{t}} \cdot \boldsymbol{\varphi}\, dA \;\to\; \text{stat.}\,, \\ \text{with} &\quad \boldsymbol{\varphi} = \bar{\boldsymbol{\varphi}} \text{ on } \partial\mathcal{B}_\varphi\,, \end{aligned} \tag{2.3}$$

and the referential density ρ_0, the given body force $\bar{\boldsymbol{b}}$ and the surface tractions $\bar{\boldsymbol{t}}$. In order to meet the objectivity condition (principle of material frame indifference) a priori, we use the well-known reduced constitutive equations in terms of the right Cauchy–Green tensor

$$\boldsymbol{C} := \boldsymbol{F}^T\boldsymbol{F}\,, \tag{2.4}$$

and put $\psi(\boldsymbol{C}) = W(\boldsymbol{F})$. The solution of (2.3) has to be computed from the condition $\delta\Pi(\boldsymbol{\varphi}, \delta\boldsymbol{\varphi}) = 0$, with the first variation of $\Pi(\boldsymbol{\varphi})$

$$\delta\Pi(\boldsymbol{\varphi}, \delta\boldsymbol{\varphi}) = \int\limits_{\mathcal{B}_0} \boldsymbol{P} \cdot \delta\boldsymbol{F}\, dV - \int\limits_{\mathcal{B}_0} \rho_0\, \bar{\boldsymbol{b}} \cdot \delta\boldsymbol{\varphi}\, dV - \int\limits_{\partial\mathcal{B}_0} \bar{\boldsymbol{t}} \cdot \delta\boldsymbol{\varphi}\, dA, \tag{2.5}$$

with

$$\boldsymbol{P} = \frac{\partial \psi(\boldsymbol{C})}{\partial \boldsymbol{F}} = \frac{\partial \psi(\boldsymbol{C})}{\partial \boldsymbol{C}} \frac{\partial \boldsymbol{C}}{\partial \boldsymbol{F}} = \boldsymbol{F}\boldsymbol{S} \quad \text{with} \quad \boldsymbol{S} = 2\frac{\partial \psi}{\partial \boldsymbol{C}}\,, \tag{2.6}$$

which yields the Euler-Lagrange equations

$$\mathrm{Div}(\boldsymbol{F}\boldsymbol{S}) + \rho_0\, \bar{\boldsymbol{b}} = \boldsymbol{0} \quad \text{and} \quad \boldsymbol{P}\bar{\boldsymbol{N}} = \bar{\boldsymbol{t}} \ \text{ on } \partial\mathcal{B}_\sigma, \tag{2.7}$$

where $\boldsymbol{P}$ and $\boldsymbol{S}$ denote the first and second Piola-Kirchhoff stress tensor, respectively. In order to guarantee the existence of solutions the underlying functional must be s.w.l.s. – this is the case if the functional is quasiconvex and satisfies the growth condition or if it is polyconvex, see Figure 1 – and must meet a coercivity condition. In the following we will focus on the construction of anisotropic polyconvex energies, because it is more tractable for the explicit evaluations of specific free energy functions than the integral inequality of the quasiconvexity condition.

3. Polyconvexity of General Anisotropic Energies.

The notion of polyconvexity – underlying the first general existence result in finite elasticity – has been introduced by Ball [1, 2].

Polyconvexity: $\boldsymbol{F} \mapsto W(\boldsymbol{F})$ is polyconvex if and only if there exists a function $P : \mathbb{R}^{3\times 3} \times \mathbb{R}^{3\times 3} \times \mathbb{R} \mapsto \mathbb{R}$ (in general non-unique) such that

$$W(\boldsymbol{F}) = P(\boldsymbol{F}, \mathrm{Cof}\boldsymbol{F}, \det\boldsymbol{F})$$

and the function $\mathbb{R}^{19} \mapsto \mathbb{R}$, $(\boldsymbol{F}, \mathrm{Cof}\boldsymbol{F}, \det\boldsymbol{F}) \mapsto P(\boldsymbol{F}, \mathrm{Cof}\boldsymbol{F}, \det\boldsymbol{F})$ is convex for all points $\boldsymbol{X} \in \mathbb{R}^3$. ■

In the above definition and in the sequel we omit the $\boldsymbol{X}$-dependence of the individual functions if there is no danger of confusion. The cofactor of $\boldsymbol{F}$ is defined by $\mathrm{Cof}\boldsymbol{F} = \det[\boldsymbol{F}]\boldsymbol{F}^{-T}$ for all invertible $\boldsymbol{F}$.

For the formulation of anisotropic hyperelastic energies further restrictions, reflecting the consequences of the principle of material symmetry, have to be taken into account. For this we have to ensure the invariance of $W(\boldsymbol{F})$ with respect to the symmetry transformations $W(\boldsymbol{F}\boldsymbol{Q})$ for all $\boldsymbol{Q} \in \mathcal{G} \subset \mathrm{O}(3)$, where $\mathcal{G}$ represents the so-called material symmetry group. Thus the reduced constitutive equations must fulfill

$$\psi(\boldsymbol{C}) = \psi(\boldsymbol{Q}\boldsymbol{C}\boldsymbol{Q}^T) \quad \forall \quad \boldsymbol{Q} \in \mathcal{G}, \tag{3.1}$$

which is the principle of material symmetry. The main idea of our proposed concept is the introduction of a structural tensor $\boldsymbol{G}$ – which can be interpreted as an anisotropic metric tensor, in the sense of a push-forward of the cartesian metric of a fictitious reference configuration onto the real reference configuration $\mathcal{B}_0$, more details are discussed in the sequel – reflecting the anisotropies of the underlying crystal class. As implied by the notion *anisotropic metric*, $\boldsymbol{G}$ has to be symmetric and positive definite. For the construction of anisotropic free energy functions we will focus on functional bases in terms of the powers of the traces of the right Cauchy-Green tensor and the tensor $\boldsymbol{G}$. Therefore we have to satisfy for the scalar products

$$\boldsymbol{C} \cdot \boldsymbol{G} = \boldsymbol{Q}\boldsymbol{C}\boldsymbol{Q}^T \cdot \boldsymbol{G} = \boldsymbol{C} \cdot \boldsymbol{Q}^T\boldsymbol{G}\boldsymbol{Q} \quad \forall\, \boldsymbol{Q} \in \mathcal{G} \subset \mathrm{O}(3). \tag{3.2}$$

Finally we must ensure the invariance requirement for the yet unknown metric tensor

$$\boldsymbol{G} = \boldsymbol{Q}\boldsymbol{G}\boldsymbol{Q}^T \quad \forall\, \boldsymbol{Q} \in \mathcal{G} \subset \mathrm{O}(3)\,; \tag{3.3}$$

thus $\boldsymbol{G}$ has to be $\mathcal{G}$-invariant. Furthermore, generic anisotropic functions of the type

$$(\mathrm{tr}[\boldsymbol{F}^T\boldsymbol{F}\boldsymbol{G}])^k = (\boldsymbol{F}^T\boldsymbol{F}\cdot\boldsymbol{G})^k \tag{3.4}$$

and

$$(\mathrm{tr}[\mathrm{Cof}[\boldsymbol{F}^T]\mathrm{Cof}[\boldsymbol{F}]\boldsymbol{G}])^k = (\mathrm{Cof}[\boldsymbol{F}^T\boldsymbol{F}]\cdot\boldsymbol{G})^k, \tag{3.5}$$

with $k \geq 1$ and $\boldsymbol{G} \in \mathrm{PSym}$ are convex with respect to the assigned arguments $\boldsymbol{F}$ and $\mathrm{Cof}\boldsymbol{F}$, respectively, and therefore polyconvex. The convexity of $(\mathrm{tr}[\boldsymbol{F}^T\boldsymbol{F}\boldsymbol{G}])^k,\ k \geq 1$ can be proved by the positivity of the second derivative. Here we exploit the fact that every symmetric, positive (semi-)definite tensor $\boldsymbol{G}$ can be written as $\boldsymbol{G} = \boldsymbol{H}\boldsymbol{H}^T$.

Proof. With the identity $(\mathrm{tr}[\boldsymbol{F}^T\boldsymbol{F}\boldsymbol{G}])^k = \|\boldsymbol{F}\boldsymbol{H}\|^{2k} = \langle\boldsymbol{F}\boldsymbol{H},\boldsymbol{F}\boldsymbol{H}\rangle^k$ we obtain

$$\begin{aligned}
D_F(\langle\boldsymbol{F}\boldsymbol{H},\boldsymbol{F}\boldsymbol{H}\rangle^k)\,.\boldsymbol{\xi} =&\ 2k\langle\boldsymbol{F}\boldsymbol{H},\boldsymbol{F}\boldsymbol{H}\rangle^{k-1}\langle\boldsymbol{F}\boldsymbol{H},\boldsymbol{\xi}\boldsymbol{H}\rangle\\
D_F^2(\langle\boldsymbol{F}\boldsymbol{H},\boldsymbol{F}\boldsymbol{H}\rangle^k)\,.(\boldsymbol{\xi},\boldsymbol{\xi}) =&\ 2k\langle\boldsymbol{F}\boldsymbol{H},\boldsymbol{F}\boldsymbol{H}\rangle^{k-1}\langle\boldsymbol{\xi}\boldsymbol{H},\boldsymbol{\xi}\boldsymbol{H}\rangle\\
&+4k(k-1)\langle\boldsymbol{F}\boldsymbol{H},\boldsymbol{F}\boldsymbol{H}\rangle^{k-2}\langle\boldsymbol{F}\boldsymbol{H},\boldsymbol{\xi}\boldsymbol{H}\rangle^2\\
=&\ 2k\,\|\boldsymbol{F}\boldsymbol{H}\|^{2k-2}\,\|\boldsymbol{\xi}\boldsymbol{H}\|^2\\
&+4k(k-1)\,\|\boldsymbol{F}\boldsymbol{H}\|^{2k-4}\ \langle\boldsymbol{F}\boldsymbol{H},\boldsymbol{\xi}\boldsymbol{H}\rangle^2 \geq 0.
\end{aligned} \tag{3.6}$$

The proof of the convexity of $(\mathrm{tr}[\mathrm{Cof}[\boldsymbol{F}^T]\mathrm{Cof}[\boldsymbol{F}]\boldsymbol{G}])^k,\ k \geq 1$ is analogous when replacing $\boldsymbol{F}$ by $\mathrm{Cof}\boldsymbol{F}$.

Since the proof of polyconvexity (3.6) is given for every $\boldsymbol{G} \in \mathrm{PSym}$ (and indeed for every symmetric and positive (semi-)definite tensor), we are now able to construct anisotropic invariants for every anisotropy class, which automatically satisfy the polyconvexity condition. We only have to insert the corresponding tensor $\boldsymbol{G} \in \mathrm{PSym}$ into (3.5).

From tensor representation theory it is well-known that using $\mathcal{G}$-invariant first and second-order structural tensors lead to complete representations for triclinic, monoclinic and rhombic symmetries as well as for transverse isotropy. For the characterization of the further usual mechanical symmetry groups higher order structural tensors are necessary: for the trigonal, tetragonal and cubic systems fourth-order and for the hexagonal systems sixth-order structural tensors are necessary, see Zheng & Spencer [48] and Zheng [47]. An analysis of the usage of second-order structural tensors for the description of the anisotropies of the 32 crystal classes is given in Xiao [45].

3.1. Generic Polyconvex Anisotropic Functions.

We construct now generic anisotropic polyconvex energy functions by using the anisotropic invariants given in (3.5). Here, we consider an additive decomposition of the free energy in isotropic and anisotropic terms, i.e.,

$$\psi = \psi^{iso}(I_1, I_2, I_3) + \psi^{aniso}(I_1, I_2, I_3, J_{4j}, J_{5j})\,. \tag{3.7}$$

Hence, the second Piola-Kirchhoff stresses consist of the two terms $\boldsymbol{S} := \boldsymbol{S}^{iso} + \boldsymbol{S}^{aniso}$:

$$\boldsymbol{S}^{iso} := 2\frac{\partial\psi^{iso}}{\partial\boldsymbol{C}} \quad \text{and} \quad \boldsymbol{S}^{aniso} := 2\frac{\partial\psi^{aniso}}{\partial\boldsymbol{C}}\,. \tag{3.8}$$

In equation (3.7) the expressions I_1, I_2 and I_3 represent the three principal invariants

$$I_1 = \mathrm{tr}\boldsymbol{C} = \boldsymbol{1}\cdot\boldsymbol{C}, \quad I_2 = \mathrm{tr}[\mathrm{Cof}\boldsymbol{C}] = \boldsymbol{1}\cdot\mathrm{Cof}\boldsymbol{C}, \quad I_3 = \det\boldsymbol{C}\,. \tag{3.9}$$

The first and second derivatives of the polyconvex base functions (3.9) are

$$\begin{aligned}
&\partial_C(\boldsymbol{1}\cdot\boldsymbol{C}) &&= \boldsymbol{1}\,, &&\partial_C^2(\boldsymbol{1}\cdot\boldsymbol{C}) &&= \boldsymbol{0}\,,\\
&\partial_C(\boldsymbol{1}\cdot\mathrm{Cof}\boldsymbol{C}) &&= I_1\boldsymbol{1} - \boldsymbol{C}\,, &&\partial_C^2(\boldsymbol{1}\cdot\mathrm{Cof}\boldsymbol{C}) &&= \boldsymbol{1}\otimes\boldsymbol{1} - \boldsymbol{1}\boxtimes\boldsymbol{1}\,,\\
&\partial_C(\det\boldsymbol{C}) &&= I_3\boldsymbol{C}^{-1}\,, &&\partial_C^2(\det\boldsymbol{C}) &&= I_3\boldsymbol{C}^{-1}\otimes\boldsymbol{C}^{-1} - I_3\boldsymbol{C}^{-1}\boxtimes\boldsymbol{C}^{-1},
\end{aligned} \tag{3.10}$$

where $\boldsymbol{A}\boxtimes\boldsymbol{B}$ denotes the tensor product of second-order tensors defined as

$$(\boldsymbol{A}\boxtimes\boldsymbol{B})(\boldsymbol{a}\otimes\boldsymbol{b}) = \boldsymbol{A}\boldsymbol{a}\otimes\boldsymbol{B}\boldsymbol{b} \qquad \forall\,\boldsymbol{A},\boldsymbol{B}\,\in\mathbb{R}^{3\times3}, \boldsymbol{a},\boldsymbol{b}\,\in\mathbb{R}^3\,, \tag{3.11}$$

see Halmos [14] and de Boer & Schröder [12]. For the isotropic part ψ^{iso} we choose a compressible Mooney-Rivlin model of the form

$$\psi^{iso} = \alpha_1\,I_1 + \alpha_2\,I_2 + \delta_1\,I_3 - \delta_2\ln(\sqrt{I_3}), \quad \forall\,\alpha_1,\ \alpha_2,\ \delta_1,\ \delta_2 \geq 0\,. \tag{3.12}$$

In detail, the isotropic part of the stress tensor is computed via

$$\boldsymbol{S}^{iso} = 2\left[\left(\frac{\partial\psi^{iso}}{\partial I_1} + \frac{\partial\psi^{iso}}{\partial I_2}I_1\right)\boldsymbol{1} - \frac{\partial\psi^{iso}}{\partial I_2}\boldsymbol{C} + \frac{\partial\psi^{iso}}{\partial I_3}I_3\boldsymbol{C}^{-1}\right]\,. \tag{3.13}$$

The remaining polyconvex base functions in the anisotropic part of (3.7) are defined as

$$J_{4j} = \mathrm{tr}[\boldsymbol{C}\boldsymbol{G}_j]\,, \qquad J_{5j} = \mathrm{tr}[\mathrm{Cof}[\boldsymbol{C}]\boldsymbol{G}_j]\,, \tag{3.14}$$

governed by the j-th metric tensor $\boldsymbol{G}_j$. Furthermore, the trace of $\boldsymbol{G}_j$ is denoted by

$$g_j := \mathrm{tr}\boldsymbol{G}_j\,. \tag{3.15}$$

The first and the second derivatives of the generic anisotropic invariants $(3.14)_1$ are

$$\partial_C(\boldsymbol{G}_j\cdot\boldsymbol{C}) = \boldsymbol{G}_j\,, \quad \partial_C^2(\boldsymbol{G}_j\cdot\boldsymbol{C}) = \boldsymbol{0}\,, \tag{3.16}$$

The derivatives of $(3.14)_2$ are given by the expressions

$$\begin{aligned}
\partial_C(\boldsymbol{G}_j\cdot\mathrm{Cof}\boldsymbol{C}) &= J_{5j}\boldsymbol{C}^{-1} - I_3\boldsymbol{C}^{-1}\boldsymbol{G}_j\boldsymbol{C}^{-1}\\
\partial_C^2(\boldsymbol{G}_j\cdot\mathrm{Cof}\boldsymbol{C}) &= J_{5j}\{\boldsymbol{C}^{-1}\otimes\boldsymbol{C}^{-1} - \boldsymbol{C}^{-1}\boxtimes\boldsymbol{C}^{-1}\}\\
&\quad -\{\mathrm{Cof}\boldsymbol{C}\otimes\boldsymbol{C}^{-1}\boldsymbol{G}_j\boldsymbol{C}^{-1} + \boldsymbol{C}^{-1}\boldsymbol{G}_j\boldsymbol{C}^{-1}\otimes\mathrm{Cof}\boldsymbol{C}\}\\
&\quad +\{\mathrm{Cof}\boldsymbol{C}\boxtimes\boldsymbol{C}^{-1}\boldsymbol{G}_j\boldsymbol{C}^{-1} + \boldsymbol{C}^{-1}\boldsymbol{G}_j\boldsymbol{C}^{-1}\boxtimes\mathrm{Cof}\boldsymbol{C}\}\,.
\end{aligned} \tag{3.17}$$

Model Problem I. Suitable anisotropic energies in terms of the yet unspecified individual polyconvex functions $f_{4r}(J_{4j}), f_{5r}(J_{5j})$ are, e.g.,

$$\psi_1^{aniso} = \sum_{r=1}^{n} \sum_{j=1}^{m} \left[f_{4r}(J_{4j}) + f_{5r}(J_{5j}) \right] . \tag{3.18}$$

For this choice we obtain $\boldsymbol{S}_1^{aniso} := 2\partial_C \psi_1^{aniso}$ with

$$\boldsymbol{S}_1^{aniso} \quad = 2 \sum_{r=1}^{n} \sum_{j=1}^{m} \left[\frac{\partial f_{5r}}{\partial J_{5j}} J_{5j} \, \boldsymbol{C}^{-1} + \frac{\partial f_{4r}}{\partial J_{4j}} \boldsymbol{G}_j - \frac{\partial f_{5r}}{\partial J_{5j}} I_3 \boldsymbol{C}^{-1} \boldsymbol{G}_j \boldsymbol{C}^{-1} \right] . \tag{3.19}$$

In order to satisfy the natural state condition of a stress-free reference configuration in the unloaded system we have to enforce $\boldsymbol{S}|_{C=1} = \boldsymbol{0}$, i.e.,

$$\begin{gathered} \left(\frac{\partial \psi^{iso}}{\partial I_1} + 2 \frac{\partial \psi^{iso}}{\partial I_2} + \frac{\partial \psi^{iso}}{\partial I_3} + \sum_{r=1}^{n} \sum_{j=1}^{m} \frac{\partial f_{5r}}{\partial J_{5j}} \, g_j \right) \boldsymbol{1} = \boldsymbol{0} , \\ \sum_{r=1}^{n} \sum_{j=1}^{m} \left[\frac{\partial f_{4r}}{\partial J_{4j}} \boldsymbol{G}_j - \frac{\partial f_{5r}}{\partial J_{5j}} \boldsymbol{G}_j \right] = \boldsymbol{0} , \end{gathered} \tag{3.20}$$

with $I_1 = 3, I_2 = 3, I_3 = 1, J_{4j} = g_j$ and $J_{5j} = g_j$ at $\boldsymbol{C} = \boldsymbol{1}$. Evaluating the special isotropic energy (3.12) at $\boldsymbol{C} = \boldsymbol{1}$ yields

$$\delta_2 = 2 \left(\alpha_1 + 2\alpha_2 + \delta_1 + \sum_{r=1}^{n} \sum_{j=1}^{m} \frac{\partial f_{5r}}{\partial J_{5j}} g_j \right) \geq 0 . \tag{3.21}$$

In general $(3.20)_2$ has to be fulfilled for each metric tensor $\boldsymbol{G}_j$ independently, thus we conclude

$$\sum_{r=1}^{n} \left[\frac{\partial f_{4r}}{\partial J_{4j}} - \frac{\partial f_{5r}}{\partial J_{5j}} \right] = 0 \quad \forall \, \boldsymbol{G}_j . \tag{3.22}$$

A further more restrictive assumption is based on the enforcement of the latter for each constant r independently, i.e.,

$$\forall \, r \ : \ f'_{4r} = f'_{5r} . \tag{3.23}$$

Model Problem II. In order to obtain a free energy representation with a decoupling between the isotropic and anisotropic material parameters we consider a set of generic polyconvex functions in terms of I_3, J_{4j} and J_{5j}. In detail we are interested in enforcing the stress-free reference configuration condition for the anisotropic energy term $\sum_{r,j} f'_{5r} g_j \boldsymbol{1}$, appearing in $(3.20)_1$, independently for each r, j. In this situation $(3.20)_1$ and (3.21) appear in the form

$$\left(\frac{\partial \psi^{iso}}{\partial I_1} + 2 \frac{\partial \psi^{iso}}{\partial I_2} + \frac{\partial \psi^{iso}}{\partial I_3} \right) \boldsymbol{1} = \boldsymbol{0} \quad \Rightarrow \quad \delta_2 = 2 \left(\alpha_1 + 2\alpha_2 + \delta_1 \right) . \tag{3.24}$$

The modification (3.24) for the condition of a stress-free reference configuration associated to the isotropic energy contributions is possible, if we choose anisotropic energies like

$$\psi_2^{aniso} = \sum_{r=1}^{n} \sum_{j=1}^{m} \left[f_{3rj}(I_3) + f_{4r}(J_{4j}) + f_{5r}(J_{5j}) \right] . \tag{3.25}$$

The second Piola-Kirchhoff stresses for the anisotropic energy contribution (3.25) denoted with $\boldsymbol{S}_2^{aniso} := 2\partial_C \psi_2^{aniso}$ are

$$\boldsymbol{S}_2^{aniso} = 2\sum_{r=1}^{n}\sum_{j=1}^{m}\left[\left(\frac{\partial f_{3rj}}{\partial I_3} I_3 + \frac{\partial f_{5r}}{\partial J_{5j}} J_{5j}\right)\boldsymbol{C}^{-1} + \frac{\partial f_{4r}}{\partial J_{4j}}\boldsymbol{G}_j - \frac{\partial f_{5r}}{\partial J_{5j}} I_3 \boldsymbol{C}^{-1}\boldsymbol{G}_j\boldsymbol{C}^{-1}\right]. \quad (3.26)$$

Let us enforce the natural state condition independently for (3.13) and (3.26). For the latter we get

$$\sum_{r=1}^{n}\sum_{j=1}^{m}\left[\left(\frac{\partial f_{3rj}}{\partial I_3} + \frac{\partial f_{5r}}{\partial J_{5j}} g_j\right)\boldsymbol{1} + \left(\frac{\partial f_{4r}}{\partial J_{4j}} - \frac{\partial f_{5r}}{\partial J_{5j}}\right)\boldsymbol{G}_j\right] = \boldsymbol{0}\,, \quad (3.27)$$

with g_j defined in (3.15). In general we conclude

$$\sum_{r=1}^{n}\sum_{j=1}^{m}\left(\frac{\partial f_{3rj}}{\partial I_3} + \frac{\partial f_{5r}}{\partial J_{5j}} g_j\right) = 0 \quad \text{and} \quad \sum_{r=1}^{n}\left(\frac{\partial f_{4r}}{\partial J_{4j}} - \frac{\partial f_{5r}}{\partial J_{5j}}\right) = 0 \quad \forall\, \boldsymbol{G}_j\,, \quad (3.28)$$

or more restrictive for all r and j independently

$$\frac{\partial f_{5r}}{\partial J_{5j}} g_j = -\frac{\partial f_{3rj}}{\partial I_3} \quad \text{and} \quad \frac{\partial f_{4r}}{\partial J_{4j}} = \frac{\partial f_{5r}}{\partial J_{5j}}\,. \quad (3.29)$$

Some specific functions which automatically satisfy (3.29) are, e.g.,

$$\begin{aligned}
f_{4r} &= \xi_{rj}\frac{1}{\alpha_{rj}+1}\frac{1}{(g_j)^{\alpha_{rj}}}(J_{4j})^{\alpha_{rj}+1} &\quad \text{with} \quad f'_{4r} &= \xi_{rj}\frac{1}{(g_j)^{\alpha_{rj}}}(J_{4j})^{\alpha_{rj}},\\
f_{5r} &= \xi_{rj}\frac{1}{\beta_{rj}+1}\frac{1}{(g_j)^{\beta_{rj}}}(J_{5j})^{\beta_{rj}+1} &\quad \text{with} \quad f'_{5r} &= \xi_{rj}\frac{1}{(g_j)^{\beta_{rj}}}(J_{5j})^{\beta_{rj}},\\
f_{3rj} &= \xi_{rj}\frac{g_j}{\gamma_{rj}}(I_3)^{-\gamma_{rj}} &\quad \text{with} \quad f'_{3rj} &= -\xi_{rj} g_j\,(I_3)^{-\gamma_{rj}-1},
\end{aligned} \quad (3.30)$$

with the parameter conditions

$$\xi_{rj} \geq 0\,, \quad \alpha_{rj} \geq 0\,, \quad \beta_{rj} \geq 0\,, \quad \gamma_{rj} \geq -1/2\,. \quad (3.31)$$

Considering (3.30) the final anisotropic energy in terms of I_3, J_{4j} and J_{5j} reads

$$\begin{aligned}
\psi_2^{aniso} = \sum_{r=1}^{n}\sum_{j=1}^{m}\xi_{rj} &\left[\frac{1}{\alpha_{rj}+1}\frac{1}{(g_j)^{\alpha_{rj}}}(J_{4j})^{\alpha_{rj}+1}\right.\\
&\left.+\frac{1}{\beta_{rj}+1}\frac{1}{(g_j)^{\beta_{rj}}}(J_{5j})^{\beta_{rj}+1} + \frac{g_j}{\gamma_{rj}}(I_3)^{-\gamma_{rj}}\right],
\end{aligned} \quad (3.32)$$

and the associated anisotropic stresses are consequently given by the expression

$$\begin{aligned}
\boldsymbol{S}_2^{aniso} = \sum_{r=1}^{n}\sum_{j=1}^{m} 2\xi_{rj} &\left[(-g_j I_3^{-\gamma_{rj}} + \frac{1}{(g_j)^{\beta_{rj}}} J_{5j}^{\beta_{rj}+1})\boldsymbol{C}^{-1} + \frac{1}{(g_j)^{\alpha_{rj}}} J_{4j}^{\alpha_{rj}}\boldsymbol{G}_j\right.\\
&\left.-\frac{1}{(g_j)^{\beta_{rj}}} J_{5j}^{\beta_{rj}} I_3 \boldsymbol{C}^{-1}\boldsymbol{G}_j\boldsymbol{C}^{-1}\right].
\end{aligned} \quad (3.33)$$

For the derivation of the material tangent tensor we introduce the abbreviation

$$\psi = \psi^{iso} + \psi_2^{aniso} \quad \text{with} \quad \psi_2^{aniso} = \sum_{r=1}^{n}\sum_{j=1}^{m} \psi_{rj}^{aniso} \tag{3.34}$$

and therefore we write in general the tangent moduli as sum of an isotropic and anisotropic part as follows

$$\mathbb{C} = 4\frac{\partial^2\psi}{\partial \boldsymbol{C}\partial \boldsymbol{C}} = 4\frac{\partial^2\psi^{iso}}{\partial \boldsymbol{C}\partial \boldsymbol{C}} + 4\sum_{r=1}^{n}\sum_{j=1}^{m}\frac{\partial^2\psi_{rj}^{aniso}}{\partial \boldsymbol{C}\partial \boldsymbol{C}} =: \mathbb{C}^{iso} + \sum_{r=1}^{n}\sum_{j=1}^{m}\mathbb{C}_{rj}^{aniso}\,. \tag{3.35}$$

In detail the isotropic part of the tangent moduli is obtained from

$$\begin{aligned}\mathbb{C}^{iso} = 4\ \Bigg[&\frac{\partial^2\psi^{iso}}{\partial I_1\partial I_1}\mathbf{1}\otimes\mathbf{1} + \frac{\partial\psi^{iso}}{\partial I_2}\ [\mathbf{1}\otimes\mathbf{1} - \mathbf{1}\boxtimes\mathbf{1}] + \frac{\partial^2\psi^{iso}}{\partial I_2\partial I_2}\{I_1\mathbf{1}-\boldsymbol{C}\}\otimes\{I_1\mathbf{1}-\boldsymbol{C}\}\\ &+\frac{\partial\psi^{iso}}{\partial I_3}\ I_3[\boldsymbol{C}^{-1}\otimes\boldsymbol{C}^{-1} - \boldsymbol{C}^{-1}\boxtimes\boldsymbol{C}^{-1}]\\ &+\frac{\partial^2\psi^{iso}}{\partial I_3\partial I_3}\mathrm{Cof}\boldsymbol{C}\otimes\mathrm{Cof}\boldsymbol{C}\Bigg]\,,\end{aligned} \tag{3.36}$$

and the anisotropic part of the material tangent tensor appears in the form

$$\begin{aligned}\mathbb{C}_{rj}^{aniso} = 4\ \Bigg[&\frac{\partial\psi_{rj}^{aniso}}{\partial I_3}\ I_3[\boldsymbol{C}^{-1}\otimes\boldsymbol{C}^{-1} - \boldsymbol{C}^{-1}\boxtimes\boldsymbol{C}^{-1}] + \frac{\partial^2\psi_{rj}^{aniso}}{\partial I_3\partial I_3}\mathrm{Cof}\boldsymbol{C}\otimes\mathrm{Cof}\boldsymbol{C}\\ &+\frac{\partial^2\psi_{rj}^{aniso}}{\partial J_{4j}\partial J_{4j}}\boldsymbol{G}_j\otimes\boldsymbol{G}_j + \frac{\partial\psi_{rj}^{aniso}}{\partial J_{5j}}\ [J_{5j}\{\boldsymbol{C}^{-1}\otimes\boldsymbol{C}^{-1} - \boldsymbol{C}^{-1}\boxtimes\boldsymbol{C}^{-1}\}\\ &\qquad - \{\mathrm{Cof}\boldsymbol{C}\otimes\boldsymbol{C}^{-1}\boldsymbol{G}_j\boldsymbol{C}^{-1} + \boldsymbol{C}^{-1}\boldsymbol{G}_j\boldsymbol{C}^{-1}\otimes\mathrm{Cof}\boldsymbol{C}\}\\ &\qquad + \{\mathrm{Cof}\boldsymbol{C}\boxtimes\boldsymbol{C}^{-1}\boldsymbol{G}_j\boldsymbol{C}^{-1} + \boldsymbol{C}^{-1}\boldsymbol{G}_j\boldsymbol{C}^{-1}\boxtimes\mathrm{Cof}\boldsymbol{C}\}]\\ &+\frac{\partial^2\psi_{rj}^{aniso}}{\partial J_{5j}\partial J_{5j}}\{J_{5j}\boldsymbol{C}^{-1} - I_3\boldsymbol{C}^{-1}\boldsymbol{G}_j\boldsymbol{C}^{-1}\}\otimes\{J_{5j}\boldsymbol{C}^{-1} - I_3\boldsymbol{C}^{-1}\boldsymbol{G}_j\boldsymbol{C}^{-1}\}\Bigg]\,,\end{aligned} \tag{3.37}$$

where we take into account that $\dfrac{\partial^2\psi}{\partial I_i\partial I_j} = \dfrac{\partial^2\psi}{\partial I_j\partial I_i}$.

Note that the anisotropic free energy function (3.32) can be used stand-alone, i.e. the free energy function given in (3.34) can be considered without the isotropic term ψ^{iso} (3.12). The reason for this lies in the fact, that (3.32) is already sufficient for satisfying the coercivity condition. The proof is given in detail in Appendix A. Furthermore, the term f_{3rj} in (3.30) can be replaced by

$$f_{3rj} = -\xi_{rj}\,\ln(I_3^{g_j}) \quad \text{with} \quad f'_{3rj} = -\xi_{rj}\frac{g_j}{I_3}\,. \tag{3.38}$$

Model Problem III. Further polyconvex functions, automatically satisfying the condition of a stress-free reference configuration, are

$$\psi_3^{aniso} = \sum_{r=1}^{n}\sum_{j=1}^{m}\left[f_{3rj}(I_3) + f_{6rj}(I_3, J_{4j}) + f_{7rj}(I_3, J_{5j})\right]\,. \tag{3.39}$$

The second Piola-Kirchhoff stresses $\boldsymbol{S}_3^{aniso} := 2\partial_C \psi_3^{aniso}$ are then given by

$$\begin{aligned}\boldsymbol{S}_3^{aniso} = 2\sum_{r=1}^{n}\sum_{j=1}^{m} & \left[\left(\frac{\partial f_{3rj}}{\partial I_3} I_3 + \frac{\partial f_{6rj}}{\partial I_3} I_3 + \frac{\partial f_{7rj}}{\partial I_3} I_3 + \frac{\partial f_{7rj}}{\partial J_{5j}} J_{5j} \right) \boldsymbol{C}^{-1} \right. \\ & \left. + \frac{\partial f_{6rj}}{\partial J_{4j}} \boldsymbol{G}_j - \frac{\partial f_{7rj}}{\partial J_{5j}} I_3 \boldsymbol{C}^{-1} \boldsymbol{G}_j \boldsymbol{C}^{-1} \right] .\end{aligned} \tag{3.40}$$

Again enforcing $\boldsymbol{S}|_{C=1} = \boldsymbol{S}^{iso}|_{C=1} + \boldsymbol{S}^{aniso}|_{C=1} = \boldsymbol{0}$ with the more restrictive assumptions $\boldsymbol{S}^{iso}|_{C=1} = \boldsymbol{0}$ and $\boldsymbol{S}^{aniso}|_{C=1} = \boldsymbol{0}$ yields for the anisotropic part

$$\begin{aligned} 2\sum_{r=1}^{n}\sum_{j=1}^{m} & \left[\left(\frac{\partial f_{3rj}}{\partial I_3} + \frac{\partial f_{6rj}}{\partial I_3} + \frac{\partial f_{7rj}}{\partial I_3} + \frac{\partial f_{7rj}}{\partial J_{5j}} g_j \right) \boldsymbol{1} \right. \\ & \left. + \left(\frac{\partial f_{6rj}}{\partial J_{4j}} - \frac{\partial f_{7rj}}{\partial J_{5j}} \right) \boldsymbol{G}_j \right] = \boldsymbol{0} .\end{aligned} \tag{3.41}$$

For the independent tensor generators $\boldsymbol{1}$ and $\boldsymbol{G}_j$ for $j = 1, ...m$ the following identities have to be satisfied

$$\frac{\partial f_{3rj}}{\partial I_3} + \frac{\partial f_{6rj}}{\partial I_3} + \frac{\partial f_{7rj}}{\partial I_3} = -\frac{\partial f_{7rj}}{\partial J_{5j}} g_j, \quad \text{and} \quad \frac{\partial f_{6rj}}{\partial J_{4j}} = \frac{\partial f_{7rj}}{\partial J_{5j}} \quad \forall\, r,\ j . \tag{3.42}$$

Some specific functions and their derivatives which automatically satisfy $(3.42)_2$ are

$$\begin{aligned} f_{6rj} &= \frac{J_{4j}^{\alpha_{rj}}}{I_3^{1/3}}, & \frac{\partial f_{6rj}}{\partial I_3} &= -\frac{1}{3}\, I_3^{-4/3} J_{4j}^{\alpha_{rj}}, & \frac{\partial f_{6rj}}{\partial J_{4j}} &= \alpha_{rj}\, J_{4j}^{\alpha_{rj}-1}\, I_3^{-1/3}, \\ f_{7rj} &= \frac{J_{5j}^{\alpha_{rj}}}{I_3^{1/3}}, & \frac{\partial f_{7rj}}{\partial I_3} &= -\frac{1}{3}\, I_3^{-4/3} J_{5j}^{\alpha_{rj}}, & \frac{\partial f_{7rj}}{\partial J_{5j}} &= \alpha_{rj}\, J_{5j}^{\alpha_{rj}-1}\, I_3^{-1/3}, \end{aligned} \tag{3.43}$$

with $\alpha_{rj} \geq 1$. For the function $f_{3rj}(I_3)$ we could use

$$f_{3rj} = \frac{g_j^{\alpha_{rj}}}{\beta_{rj}}\, I_3^{-\beta_{rj}}, \quad \frac{\partial f_{3rj}}{\partial I_3} = -g_j^{\alpha_{rj}}\, I_3^{-\beta_{rj}-1}, \quad \text{with} \quad \beta_{rj} \geq -1/2\, ; \tag{3.44}$$

inserting (3.43) and (3.44) into $(3.42)_1$ leads directly to the material parameter α_{rj}, i.e.,

$$\alpha_{rj} = \frac{5}{3} . \tag{3.45}$$

Alternatively we can consider the function

$$f_{3rj} = -g_j^{\alpha_{rj}}\, \beta_{rj}\, \ln(I_3)\, , \qquad \frac{\partial f_{3rj}}{\partial I_3} = -\beta_{rj}\, \frac{g_j^{\alpha_{rj}}}{I_3} \quad \text{with} \quad \alpha_{rj} \geq 1\, ; \tag{3.46}$$

using (3.43) and (3.46) in $(3.42)_1$ we obtain the restriction

$$\beta_{rj} = \alpha_{rj} - \frac{2}{3} . \tag{3.47}$$

In order to compute the complete tangent moduli we must add

$$
\begin{aligned}
4\sum_{r=1}^{n}\sum_{j=1}^{m} \Bigg[& \frac{\partial^2 \psi_{rj}^{aniso}}{\partial I_3 \partial J_{4j}} [\mathrm{Cof}\boldsymbol{C} \otimes \boldsymbol{G}_j + \boldsymbol{G}_j \otimes \mathrm{Cof}\boldsymbol{C}] \\
& + \frac{\partial^2 \psi_{rj}^{aniso}}{\partial I_3 \partial J_{5j}} [\mathrm{Cof}\boldsymbol{C} \otimes \{J_{5j}\boldsymbol{C}^{-1} - I_3 \boldsymbol{C}^{-1}\boldsymbol{G}_j\boldsymbol{C}^{-1}\} \\
& + \{J_{5j}\boldsymbol{C}^{-1} - I_3 \boldsymbol{C}^{-1}\boldsymbol{G}_j\boldsymbol{C}^{-1}\} \otimes \mathrm{Cof}\boldsymbol{C}]\Bigg]
\end{aligned}
\tag{3.48}
$$

to the expression given in (3.35).

Based on the aforementioned analysis of different anisotropic polyconvex energies we summarize four suitable explicit functions in Table 1. For the orthotropic case we also refer in this context to [16].

Table 1: Four Different Polyconvex Anisotropic Energy Functions Satisfying Stress-Free Reference Configuration Condition

$$
\begin{aligned}
\psi_I^{aniso} = \sum_{r=1}^{n}\sum_{j=1}^{m} \xi_{rj} \Bigg[& \frac{1}{\alpha_{rj}+1}\frac{1}{(g_j)^{\alpha_{rj}}}(J_{4j})^{\alpha_{rj}+1} \\
& + \frac{1}{\beta_{rj}+1}\frac{1}{(g_j)^{\beta_{rj}}}(J_{5j})^{\beta_{rj}+1} + \frac{g_j}{\gamma_{rj}}(I_3)^{-\gamma_{rj}}\Bigg]
\end{aligned}
$$

with $\xi_{rj} \geq 0\,, \quad \alpha_{rj} \geq 0\,, \quad \beta_{rj} \geq 0\,, \quad \gamma_{rj} \geq -1/2$

$$
\begin{aligned}
\psi_{II}^{aniso} = \sum_{r=1}^{n}\sum_{j=1}^{m} \xi_{rj} \Bigg[& \frac{1}{\alpha_{rj}+1}\frac{1}{(g_j)^{\alpha_{rj}}}(J_{4j})^{\alpha_{rj}+1} \\
& + \frac{1}{\beta_{rj}+1}\frac{1}{(g_j)^{\beta_{rj}}}(J_{5j})^{\beta_{rj}+1} - \ln(I_3^{g_j})\Bigg]
\end{aligned}
$$

with $\xi_{rj} \geq 0\,, \quad \alpha_{rj} \geq 0\,, \quad \beta_{rj} \geq 0$

$$
\psi_{III}^{aniso} = \sum_{r=1}^{n}\sum_{j=1}^{m} \left[\frac{J_{4j}^{\alpha_{rj}}}{I_3^{1/3}} + \frac{J_{5j}^{\alpha_{rj}}}{I_3^{1/3}} + \frac{g_j^{\alpha_{rj}}}{\beta_{rj}}\; I_3^{-\beta_{rj}} \right]
$$

with $\alpha_{rj} = 5/3\,, \quad \beta_{rj} \geq -1/2$

$$
\psi_{IV}^{aniso} = \sum_{r=1}^{n}\sum_{j=1}^{m} \left[\frac{J_{4j}^{\alpha_{rj}}}{I_3^{1/3}} + \frac{J_{5j}^{\alpha_{rj}}}{I_3^{1/3}} - g_j^{\alpha_{rj}}\; \beta_{rj}\, \ln(I_3) \right]
$$

with $\alpha_{rj} \geq 1\,, \quad \beta_{rj} = \alpha_{rj} - 2/3$

3.2. Metric Tensors for the Seven Crystal Systems.

The symmetry of crystals as well as their anisotropic physical properties are closely related to the so-called crystal lattices. A lattice can be carried into itself by suitable translations of the basic periods of the crystal lattice. These periodic cells are the (not uniquely determined) 14 types of Bravais lattices, which are associated with seven crystal systems. A Bravais lattice is determined by three base vectors $\boldsymbol{a}_1, \boldsymbol{a}_2, \boldsymbol{a}_3$, with $a = ||\boldsymbol{a}_1||, b = ||\boldsymbol{a}_2||, c = ||\boldsymbol{a}_3||$ and the axial angles α, β, γ, see Figure 3.

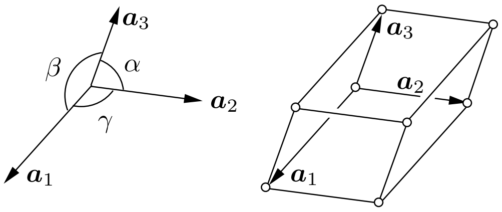

Figure 3: Bravais lattice with base vectors $\boldsymbol{a}_1, \boldsymbol{a}_2, \boldsymbol{a}_3$ and axial angles α, β, γ.

For the case of anisotropic elasticity there exist 12 types of symmetry groups. Eleven of them characterize the 32 crystal classes and the remaining one describes the transversely isotropic case, see Şuhubi [44], Smith & Rivlin [39, 40], Smith, Smith & Rivlin [41], Spencer [42] and Liu [19] and the references therein. The material symmetries of a considered crystal imposes restrictions on the physical coefficients. Relations between symmetries of a crystal and its physical properties are postulated by the fundamental Neumann principle [29]:

Symmetry elements associated with any physical property of a crystal must include those of the symmetry point group of the crystal.

Note that the physical properties may have a greater symmetry than the associated point group of the crystal. However, the symmetry of the physical properties cannot be lower than that of the crystal. Crystals can be classified in seven systems, see Table 2.

Table 2: The seven crystal systems

No.	crystal system	edge lengths	axial angle
1	triclinic	$a \neq b \neq c$	$\alpha \neq \beta \neq \gamma \neq 90°$
2	monoclinic	$a \neq b \neq c$	$\alpha = \beta = 90°;\ \gamma \neq 90°$
3	trigonal	$a = b = c$	$\alpha = \beta = \gamma \neq 90°$
4	hexagonal	$a = b \neq c$	$\alpha = \beta = 90°;\ \gamma = 120°$
5	rhombic	$a \neq b \neq c$	$\alpha = \beta = \gamma = 90°$
6	tetragonal	$a = b \neq c$	$\alpha = \beta = \gamma = 90°$
7	cubic	$a = b = c$	$\alpha = \beta = \gamma = 90°$

In the following we are interested in the construction of a second-order tensor $\boldsymbol{G}$, which reflects the basic symmetry relations of the considered crystal class. In analogy to Menzel

& Steinmann [23] we introduce a fictitious reference configuration $\bar{\mathcal{B}}_0$. Let $\boldsymbol{H}$ represent a linear tangent map, which maps cartesian base vectors $\bar{\boldsymbol{e}}_i \in \bar{\mathcal{B}}_0$ onto crystallographic motivated base vectors $\boldsymbol{a}_i \in \mathcal{B}_0$, i.e. $\boldsymbol{H} : \bar{\boldsymbol{e}}_i \mapsto \boldsymbol{a}_i$. In this context $\boldsymbol{G} = \boldsymbol{H}\boldsymbol{H}^T$ can be considered as a push-forward of the cartesian metric of the fictitious configuration $\bar{\mathcal{B}}_0$. It should be noted that the introduced second-order tensors can be interpreted as the so-called structural tensors introduced by Boehler [7, 8, 9] and Liu [19] in some sense. The main difference here is the required positive definiteness of $\boldsymbol{G}$, necessary for the polyconvexity condition (slight modifications in the aforementioned analysis also allow positive semi-definite tensors $\boldsymbol{G}$). For the extension of the $\mathcal{G}$-invariant functions into functions which are invariant under the orthogonal group, the required additional structural tensors are of order up to six, see Zhang & Rychlewski [46], Zheng & Spencer [48] and Zheng [47]. Therefore it is clear that our ansatz cannot reflect the whole collections of invariants required for a complete description of the underlying anisotropies of some crystal classes. Nevertheless the restricted approach satisfies the fundamental existence theories in finite elasticity.

For the construction of the inherent anisotropic metric $\boldsymbol{G}$ we consider a transformation matrix $\boldsymbol{H}$, which can be interpreted as an initial mapping of the cartesian base system $\bar{\boldsymbol{e}}_1 = (1,0,0)^T$, $\bar{\boldsymbol{e}}_2 = (0,1,0)^T$, $\bar{\boldsymbol{e}}_3 = (0,0,1)^T$. The transformation of the cartesian base vectors to the crystallographic base system related to the associated Bravais lattice are expressed by

$$\boldsymbol{H} = [\boldsymbol{a}_1, \boldsymbol{a}_2, \boldsymbol{a}_3] \quad \text{with} \quad \boldsymbol{a}_i = \boldsymbol{H}\,\bar{\boldsymbol{e}}_i \,. \tag{3.49}$$

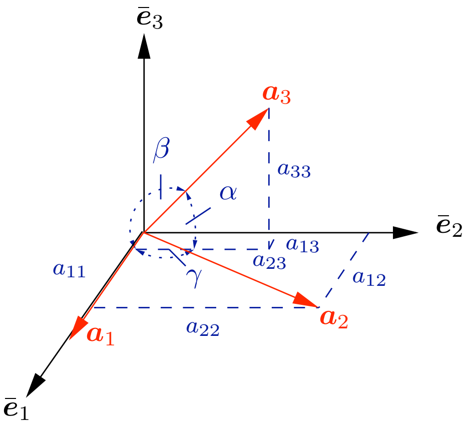

Figure 4: Geometrical interpretation of the six components of $\boldsymbol{H}$ given in (3.50).

The coefficient scheme of the transformation $\boldsymbol{H}$ has in general nine non-vanishing entries; six of them are necessary for the classification of the crystal system and the remaining three are used to describe the relative orientation of the crystallographic base systems with respect to the underlying cartesian one. In the following analysis it is sufficient to concentrate on the different crystal systems only. Therefore we make special choices for the orientations of the base vectors: for example we set $\boldsymbol{a}_1 \parallel \bar{\boldsymbol{e}}_1$ and $\boldsymbol{a}_2 \perp \bar{\boldsymbol{e}}_3$. This leads to the following representation of the tensor $\boldsymbol{H}$

$$\boldsymbol{H} = \begin{bmatrix} a_{11} & a_{12} & a_{13} \\ 0 & a_{22} & a_{23} \\ 0 & 0 & a_{33} \end{bmatrix} . \tag{3.50}$$

The geometric interpretation of the components of the upper triangular matrix $\boldsymbol{H}$ – for the above mentioned relative orientation of the base systems – is depicted in Figure 4. The angles are given by the relations

$$\cos\alpha = \frac{\boldsymbol{a}_2 \cdot \boldsymbol{a}_3}{\parallel \boldsymbol{a}_2 \parallel \, \parallel \boldsymbol{a}_3 \parallel}\,, \quad \cos\beta = \frac{\boldsymbol{a}_3 \cdot \boldsymbol{a}_1}{\parallel \boldsymbol{a}_3 \parallel \, \parallel \boldsymbol{a}_1 \parallel}\,, \quad \cos\gamma = \frac{\boldsymbol{a}_1 \cdot \boldsymbol{a}_2}{\parallel \boldsymbol{a}_1 \parallel \, \parallel \boldsymbol{a}_2 \parallel}\,. \tag{3.51}$$

Substituting the lengths a, b, c of the individual crystallographic base vectors $\boldsymbol{a}_1, \boldsymbol{a}_2$ and $\boldsymbol{a}_3$, respectively, and (3.51) into (3.50) yields

$$\boldsymbol{H} = \begin{bmatrix} a & b\,\cos\gamma & c\,\cos\beta \\ 0 & b\,\sin\gamma & c\,(\cos\alpha - \cos\beta\,\cos\gamma)/\sin\gamma \\ 0 & 0 & c\,[1 + 2\,\cos\alpha\,\cos\beta\,\cos\gamma - \\ & & (\cos^2\alpha + \cos^2\beta + \cos^2\gamma)]^{1/2}/\sin\gamma \end{bmatrix}. \tag{3.52}$$

For the seven systems we choose the metric representations presented in Table 3.

Table 3: Metric representations $\boldsymbol{G} = \boldsymbol{H}\boldsymbol{H}^T$

Triclinic system with $\boldsymbol{a}_1 \parallel \bar{\boldsymbol{e}}_1$ and $\boldsymbol{a}_2 \perp \bar{\boldsymbol{e}}_3$:
$\boldsymbol{H}^a = \begin{bmatrix} a_{11} & a_{12} & a_{13} \\ 0 & a_{22} & a_{23} \\ 0 & 0 & a_{33} \end{bmatrix}, \quad \boldsymbol{G}^a = \begin{bmatrix} \tilde{a} & \tilde{d} & \tilde{e} \\ \tilde{d} & \tilde{b} & \tilde{f} \\ \tilde{e} & \tilde{f} & \tilde{c} \end{bmatrix},$ with $\tilde{a} = a^2 + b^2\,\cos^2\gamma + c^2\,\cos^2\beta$ $\tilde{b} = b^2\,\sin^2\gamma + \dfrac{c^2\,(\cos\alpha - \cos\beta\,\cos\gamma)^2}{\sin^2\gamma}$ $\tilde{c} = \dfrac{c^2(1 + 2\,\cos\alpha\,\cos\beta\,\cos\gamma - \cos^2\alpha - \cos^2\beta - \cos^2\gamma)}{\sin^2\gamma}$ $\tilde{d} = b^2\cos\gamma\,\sin\gamma + \dfrac{c^2\cos\beta\,(\cos\alpha - \cos\beta\,\cos\gamma)}{\sin\gamma}$ $\tilde{e} = \dfrac{c^2\cos\beta\,(1 + 2\,\cos\alpha\,\cos\beta\cos\gamma - \cos^2\alpha - \cos^2\beta - \cos^2\gamma)^{1/2}}{\sin\gamma}$ $\tilde{f} = \dfrac{c^2(\cos\alpha - \cos\beta\,\cos\gamma)\,(1 + 2\,\cos\alpha\,\cos\beta\cos\gamma - \cos^2\alpha - \cos^2\beta - \cos^2\gamma)^{1/2}}{\sin^2\gamma}$
Monoclinic system with $\boldsymbol{a}_1 \parallel \bar{\boldsymbol{e}}_1$ and $\boldsymbol{a}_3 \parallel \bar{\boldsymbol{e}}_3$:
$\boldsymbol{H}^m = \begin{bmatrix} a & b\,\cos\gamma & 0 \\ 0 & b\,\sin\gamma & 0 \\ 0 & 0 & c \end{bmatrix}, \quad \boldsymbol{G}^m = \begin{bmatrix} a^2 + b^2\,\cos^2\gamma & b^2\,\cos\gamma\,\sin\gamma & 0 \\ b^2\cos\gamma\,\sin\gamma & b^2\,\sin^2\gamma & 0 \\ 0 & 0 & c^2 \end{bmatrix}$

Trigonal system: Rhombohedral system with $(\boldsymbol{a}_1 + \boldsymbol{a}_2 + \boldsymbol{a}_3) \parallel \bar{\boldsymbol{e}}_3$, see Figure 5:

$$\boldsymbol{H}^h = \begin{bmatrix} 1/\sqrt{3}\,a & -1/(2\sqrt{3})\,a & -1/(2\sqrt{3})\,a \\ 0 & 1/2\,a & -1/2\,a \\ c/3 & c/3 & c/3 \end{bmatrix}, \quad \boldsymbol{G}^h = \begin{bmatrix} a^2/2 & 0 & 0 \\ 0 & a^2/2 & 0 \\ 0 & 0 & c^2/3 \end{bmatrix}$$

Hexagonal system with $\boldsymbol{a}_i \parallel \bar{\boldsymbol{e}}_i,\ a = b \neq c$ (see the forthcoming remarks):

$$\boldsymbol{H}^{ht} = \begin{bmatrix} a & 0 & 0 \\ 0 & a & 0 \\ 0 & 0 & c \end{bmatrix}, \quad \boldsymbol{G}^{ht} = \begin{bmatrix} a^2 & 0 & 0 \\ 0 & a^2 & 0 \\ 0 & 0 & c^2 \end{bmatrix}$$

Rhombic system with $\boldsymbol{a}_i \parallel \bar{\boldsymbol{e}}_i$:

$$\boldsymbol{H}^o = \begin{bmatrix} a & 0 & 0 \\ 0 & b & 0 \\ 0 & 0 & c \end{bmatrix}, \quad \boldsymbol{G}^o = \begin{bmatrix} a^2 & 0 & 0 \\ 0 & b^2 & 0 \\ 0 & 0 & c^2 \end{bmatrix}$$

Tetragonal system with $\boldsymbol{a}_i \parallel \bar{\boldsymbol{e}}_i$:

$$\boldsymbol{H}^t = \begin{bmatrix} a & 0 & 0 \\ 0 & a & 0 \\ 0 & 0 & c \end{bmatrix}, \quad \boldsymbol{G}^t = \begin{bmatrix} a^2 & 0 & 0 \\ 0 & a^2 & 0 \\ 0 & 0 & c^2 \end{bmatrix}$$

Cubic system with $\boldsymbol{a}_i \parallel \bar{\boldsymbol{e}}_i$:

$$\boldsymbol{H}^c = \begin{bmatrix} a & 0 & 0 \\ 0 & a & 0 \\ 0 & 0 & a \end{bmatrix}, \quad \boldsymbol{G}^c = \begin{bmatrix} a^2 & 0 & 0 \\ 0 & a^2 & 0 \\ 0 & 0 & a^2 \end{bmatrix}$$

Now we check the consequences of the approach with respect to the well-known representations of anisotropic energy functions. Therefore we evaluate the terms $\boldsymbol{C} \cdot \boldsymbol{G}$ and $\mathrm{Cof}\boldsymbol{C} \cdot \boldsymbol{G}$ and identify the coefficients of the independent components of $\boldsymbol{G}$. These coefficients reflect the inherent (maybe incomplete) functional bases of the considered crystal class up to the power of two. The integrity bases for a single, symmetric, second-order, three-dimensional tensor for each of the 32 crystal classes have been determined in Smith & Rivlin [40], see also Smith & Rivlin [39] and Şuhubi [44].

Triclinic system: Evaluating $\boldsymbol{C} \cdot \boldsymbol{G}^a$ and $\mathrm{Cof}\boldsymbol{C} \cdot \boldsymbol{G}^a$ yields, after ordering with respect to the individual entries $\tilde{a}, \tilde{b}, \tilde{c}, \tilde{d}, \tilde{e}, \tilde{f}$ in $\boldsymbol{G}^a$, the functional basis

$$C_{11}\,,\ C_{22}\,,\ C_{33}\,,\ C_{12}\,,\ C_{13}\,,\ C_{23} \tag{3.53}$$

and identical components in terms of the cofactor of $\boldsymbol{C}$. Equation (3.53) represents the full functional basis for the triclinic class.

Monoclinic system: Examining the scalar products $\boldsymbol{C} \cdot \boldsymbol{G}^m$ and $\mathrm{Cof}\boldsymbol{C} \cdot \boldsymbol{G}^m$ leads to the elements

$$C_{11}\,,\ C_{22}\,,\ C_{33}\,,\ C_{12} \tag{3.54}$$

and

$$\begin{aligned}
\mathrm{Cof}C_{11} &= C_{22}C_{33} - C_{23}^2\,,\\
\mathrm{Cof}C_{22} &= C_{11}C_{33} - C_{13}^2\,,\\
\mathrm{Cof}C_{33} &= C_{11}C_{22} - C_{12}^2\,,\\
\mathrm{Cof}C_{12} &= C_{13}C_{23} - C_{12}C_{33}\,,
\end{aligned} \tag{3.55}$$

respectively. The full functional basis of the monoclinic class is given by the well-known representation

$$C_{11}\,,\ C_{22}\,,\ C_{33}\,,\ C_{12}\,,\ C_{13}^2\,,\ C_{23}^2\,,\ C_{13}\,C_{23}\,. \tag{3.56}$$

A comparison of (3.54) and (3.55) with (3.56) shows that all elements of the classical basis (3.56) appear in the polyconvex framework, but in a non-trivial sense.

Trigonal system: Let $\boldsymbol{a}_h, \boldsymbol{b}_h, \boldsymbol{c}_h$ be the basis of the hexagonal centered cell, with the threefold axis $\boldsymbol{c}_h \parallel \bar{\boldsymbol{e}}_3$. The basis of the associated rhombohedral cell is denoted by $\boldsymbol{a}_1, \boldsymbol{a}_2, \boldsymbol{a}_3$ of equal lengths:

$$\boldsymbol{a}_1 = \frac{1}{3}(2\boldsymbol{a}_h + \boldsymbol{b}_h + \boldsymbol{c}_h)\,,\quad \boldsymbol{a}_2 = \frac{1}{3}(-\boldsymbol{a}_h + \boldsymbol{b}_h + \boldsymbol{c}_h)\,,\quad \boldsymbol{a}_3 = \frac{1}{3}(-\boldsymbol{a}_h - 2\boldsymbol{b}_h + \boldsymbol{c}_h)\,,$$

with the threefold axis along the $(\boldsymbol{a}_1 + \boldsymbol{a}_2 + \boldsymbol{a}_3)$-direction.

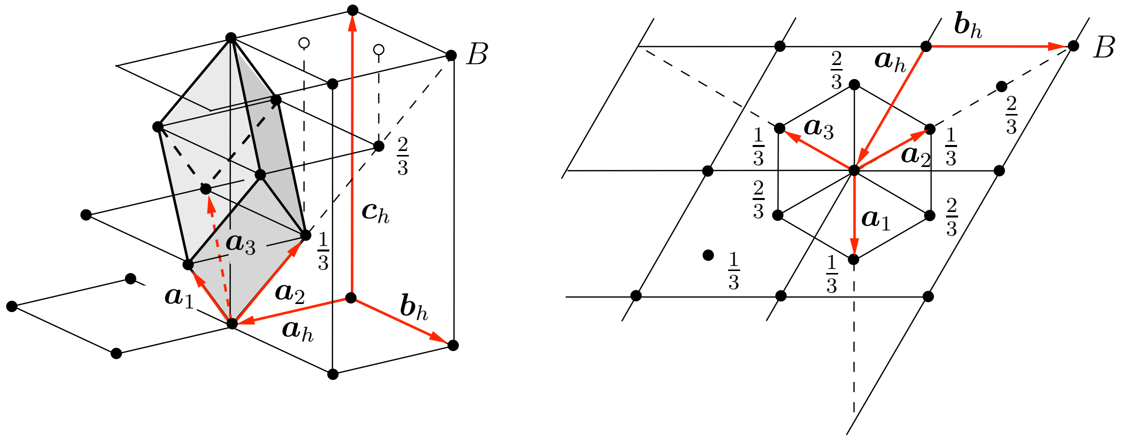

Figure 5: Primitive cell of rhombohedral shape.

These geometrical crystallographic relations lead to the transformation matrix $\boldsymbol{H}$ and the second-order tensor $\boldsymbol{G}^h$ listed in Table 3. After ordering the terms of $\boldsymbol{C}\cdot\boldsymbol{G}^h$ and $\mathrm{Cof}\,\boldsymbol{C}\cdot\boldsymbol{G}^h$ with respect to the individual components of $\boldsymbol{G}^h$, we obtain the elements of the functional basis

$$\begin{aligned}
&C_{11} + C_{22}\,,\ C_{33}\,,\\
\mathrm{Cof}C_{11} + \mathrm{Cof}C_{22} &= C_{22}C_{33} + C_{11}C_{33} - (C_{23}^2 + C_{13}^2)\,,\\
\mathrm{Cof}C_{33} &= C_{11}C_{22} - C_{12}^2\,.
\end{aligned} \tag{3.57}$$

A comparison of the scalar invariants (3.57) with the functional basis of independent scalar invariants of the trigonal (rhombohedral) system with seven independent elasticities $\mathbb{C}_{ijkl}$ of the fourth-order linearized elasticity tensor $\mathbb{C}$

$$\begin{gathered} C_{11}+C_{22}\,, \quad C_{33}\,, \quad C_{13}^2+C_{23}^2\,, \quad C_{11}^2+C_{22}^2+2\,C_{12}^2\,, \\ C_{13}(C_{11}-C_{22})-2\,C_{12}C_{23}\,, \quad C_{23}(C_{11}-C_{22})+2\,C_{12}C_{13}\,, \end{gathered} \tag{3.58}$$

given in Dimitrienko [13], shows that the last two invariants in the set (3.58) cannot be expressed by simple combinations of the terms appearing in the polyconvex framework (3.57). In the trigonal system with six independent elasticities the last invariant in (3.58) has to be replaced by $\det\boldsymbol{C}$, which is always an element of the proposed functional basis.

Hexagonal system: A primitive hexagonal cell can be described by two base vectors $\boldsymbol{a}_H$ and $\boldsymbol{b}_H$ lying in the $\bar{\boldsymbol{e}}_1-\bar{\boldsymbol{e}}_2$–plane and a third vector perpendicular to this lattice plane. In order to capture the inherent symmetries of this lattice Bravais (1866) introduced a third (redundant) base vector $\boldsymbol{c}_H=-\boldsymbol{a}_H-\boldsymbol{b}_H$ in the $\bar{\boldsymbol{e}}_1-\bar{\boldsymbol{e}}_2$–plane. All vectors $\boldsymbol{a}_H$, $\boldsymbol{b}_H$, $\boldsymbol{c}_H$ are equivalent. Reflections with respect to planes perpendicular to these privileged directions show the inherent sixfold symmetry. This is related to rotations through 60° about the $\bar{\boldsymbol{e}}_3$-axis, which indicates that the $\bar{\boldsymbol{e}}_1-\bar{\boldsymbol{e}}_2$–plane acts as an isotropy plane, see Love [20]. Therefore the fictitious deformation has to be of the type

$$\boldsymbol{H}^{ht}=\operatorname{diag}(a,a,c) \quad \rightarrow \quad \boldsymbol{G}^{ht}=\operatorname{diag}(a^2,a^2,c^2)\,. \tag{3.59}$$

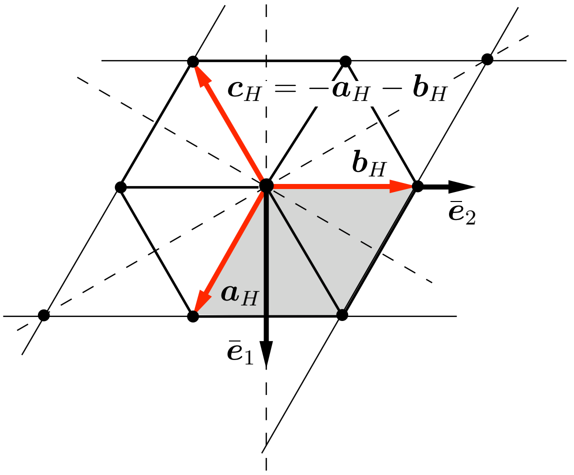

Figure 6: Hexagonal lattice of a primitive hexagonal cell.

The anisotropic invariants in the proposed approach are identical to (3.57) and after including $\det\boldsymbol{C}$ it is equivalent to the full functional basis given in [13].

Tetragonal system: For the tetragonal system we also obtain the anisotropic invariants (3.57), which, however, do not reflect the complete functional basis.

Rhombic system: Performing the same analysis as above we get the basis of anisotropic invariants in the polyconvex framework:

$$C_{11}\,,\ C_{22}\,,\ C_{33}\,,\ \operatorname{Cof}C_{11}\,,\ \operatorname{Cof}C_{22}\,,\ \operatorname{Cof}C_{33}\,, \tag{3.60}$$

which is complete after adding $\det\boldsymbol{C}$, see section 3.5.

Cubic system: Up to the power of two we only obtain the anisotropic invariants tr$\boldsymbol{C}$ and tr[Cof $\boldsymbol{C}$] instead of three, which only represent the isotropic invariants of the right Cauchy-Green tensor.

3.3. Anisotropic Moduli–Fitting to Referential Data.

In order to approximate the phenomenological responses of real anisotropic materials with the above mentioned anisotropic polyconvex functions we have to fit the stress-strain relation to experimental measurements or alternatively we have to fit the fourth-order elasticity tensor near the natural state to some available data. An adjustment of two superimposed transversely isotropic response functions to experimental data of overstretched arterial walls as well as an accompanying localization analysis are discussed in Balzani, Neff, Schröder & Holzapfel [6] and Balzani [5].

In the following we focus on the fitting of the linearized fourth-order elasticity tensor $\mathbb{C}_0$ to some experimental measurements. A huge variety of data are available in Simmons & Wang [38]. Let us consider the linearized stress-strain relation near the reference configuration; thus, the linearized moduli $\mathbb{C}_0$ at the reference state result from the linearization of the stress response functions at a natural state, i.e.,

$$Lin[\boldsymbol{S}] = \mathbb{C}_0 : Lin[\boldsymbol{E}] \quad \text{with} \quad \mathbb{C}_0 := 2\frac{\partial \boldsymbol{S}}{\partial \boldsymbol{C}}\bigg|_{C=1} \quad \text{and} \quad \boldsymbol{S}|_{C=1} = \boldsymbol{0} \tag{3.61}$$

and the Green-Lagrange strain tensor

$$\boldsymbol{E} := \frac{1}{2}(\boldsymbol{C} - \boldsymbol{1})\,. \tag{3.62}$$

The term $Lin[\boldsymbol{S}]$ can be identified with the linear stress tensor $\boldsymbol{\sigma}$ and the term $Lin[\boldsymbol{E}]$ with the linear strain tensor $\boldsymbol{\varepsilon}$ in the small strain regime. Thus, (3.61) reduces to the linear relation $\boldsymbol{\sigma} = \mathbb{C}_0 : \boldsymbol{\varepsilon}$. Hence, we identify the material parameters by comparing the calculated tangent moduli with experimental data based moduli given in the classical representation. In detail, the fitting of moduli is done by minimizing the error function

$$e = \frac{\parallel \mathbb{C}^{(V)comp} - \mathbb{C}^{(V)exp} \parallel}{\parallel \mathbb{C}^{(V)exp} \parallel}\,. \tag{3.63}$$

Here $\mathbb{C}^{(V)comp} \in \mathbb{R}^{6\times 6}$ denotes the computed tangent moduli $\mathbb{C}_0$ in Voigt notation. Furthermore, $\mathbb{C}^{(V)exp} \in \mathbb{R}^{6\times 6}$ is the associated coefficient scheme of experimental values. The used norm of the matrix schemes are defined by

$$\parallel \mathbb{C}^{(V)} \parallel = \sqrt{\sum_{i=1}^{6}\sum_{j=1}^{6}(\mathbb{C}_{ij}^{(V)})^2}\,. \tag{3.64}$$

The performed parameter adjustments have been done with the evolution strategy proposed by Schwefel [35] and Rechenberg [30]. Furthermore, we plot the characteristic surfaces of Young's modulus for the adjusted elasticities to visualize the anisotropy ratios, see Shuvalov [36].

3.3.1. Monoclinic System. As an example for the fitting described above, we are interested in the approximation of a monoclinic material. The elasticity moduli for the monoclinic material Aegirite as well as the characteristic surface of Young's moduli are depicted in Figure 7, parameters are taken from Simmons & Wang [38].

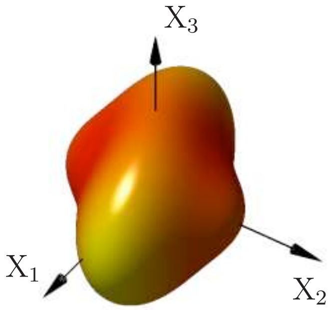

$$\mathbb{C}^{(V)} = \begin{bmatrix} 234.4 & 70.7 & 62.6 & 21.4 & 0 & 0 \\ & 185.8 & 68.5 & 9.8 & 0 & 0 \\ & & 181.3 & 9.4 & 0 & 0 \\ & & & 51.0 & 0 & 0 \\ & sym. & & & 47.4 & 7.7 \\ & & & & & 69.2 \end{bmatrix}$$

Figure 7: Monoclinic material: characteristic surface of Young's modulus, elasticities [GPa].

The material parameters of the free energy function given in (3.34) are first fitted. Remember therefore that this free energy function is of the type

$$\psi = \psi^{iso} + \psi_2^{aniso} \,, \tag{3.65}$$

with the compressible Mooney-Rivlin model (3.12) and the anisotropic part

$$\begin{aligned} \psi_2^{aniso} = \sum_{r=1}^{n}\sum_{j=1}^{m} \xi_{rj} \quad & \left[\frac{1}{\alpha_{rj}+1}\frac{1}{(g_j)^{\alpha_{rj}}}(J_{4j})^{\alpha_{rj}+1} \right. \\ & \left. + \frac{1}{\beta_{rj}+1}\frac{1}{(g_j)^{\beta_{rj}}}(J_{5j})^{\beta_{rj}+1} + \frac{g_j}{\gamma_{rj}}(I_3)^{-\gamma_{rj}} \right] , \end{aligned} \tag{3.66}$$

where the parameter conditions (3.31) must be fulfilled. Setting the summation index $n = m = 2$ and using the representation of a monoclinic metric tensor

$$\boldsymbol{G}_j^m = \begin{bmatrix} a_j & d_j & 0 \\ d_j & b_j & 0 \\ 0 & 0 & c_j \end{bmatrix} \quad \text{with} \quad a_j \,,\; c_j > 0 \,,\; d_j^2 \;<\; a_j\, b_j \,, \tag{3.67}$$

yields the material parameters for the isotropic part

$$\alpha_1 = 3.925 \,,\; \alpha_2 = 0 \,,\; \delta_1 = 0.072 \,,\; \delta_2 = 7.994 \,, \tag{3.68}$$

and the parameters for the anisotropic contributions listed in Table 4. The monoclinic metric tensors appear in the form

$$\boldsymbol{G}_1^m = \begin{bmatrix} 1.570 & -0.142 & 0 \\ -0.142 & 0.040 & 0 \\ 0 & 0 & 1.808 \end{bmatrix} , \quad \boldsymbol{G}_2^m = \begin{bmatrix} 2.599 & 0.455 & 0 \\ 0.455 & 0.749 & 0 \\ 0 & 0 & 2.008 \end{bmatrix} . \tag{3.69}$$

Table 4: Material parameter set I for Aegirite

r	j	α_{rj}	β_{rj}	γ_{rj}	ξ_{rj}
1	1	0.233	3.221	-0.465	1.407
1	2	3.067	0.105	-0.474	0.598
2	2	4.287	0.0000017	-0.468	5.345
2	1	0.148	3.026	-0.486	0.00005

Consequently the fitted monoclinic anisotropic tangent modulus reads

$$\mathbb{C}^{(V)comp} = \begin{bmatrix} 233.71 & 70.97 & 62.97 & 22.08 & 0 & 0 \\ & 185.82 & 68.18 & 9.38 & 0 & 0 \\ & & 181.32 & 8.61 & 0 & 0 \\ & & & 53.81 & 0 & 0 \\ & sym. & & & 44.73 & 4.30 \\ & & & & & 70.66 \end{bmatrix}, \tag{3.70}$$

which gives a relative error of $e = 1.65\%$, see (3.63).

Let us now fit the elasticities (see Figure 7) using the free energy function $\psi = \psi_2^{aniso}$, i.e. we here neglect the isotropic Mooney-Rivlin part. In the following analysis we increase the number of generating terms by setting $n = m = 3$; furthermore, we set $\boldsymbol{G}_1 = \mathrm{diag}(1, 1, 1)$. After the optimization the remaining anisotropic metric tensors appear in the form

$$\boldsymbol{G}_2^m = \begin{bmatrix} 2.530 & 0.433 & 0 \\ 0.433 & 0.676 & 0 \\ 0 & 0 & 1.976 \end{bmatrix}, \quad \boldsymbol{G}_3^m = \begin{bmatrix} 2.218 & -0.228 & 0 \\ -0.228 & 0.218 & 0 \\ 0 & 0 & 2.596 \end{bmatrix}. \tag{3.71}$$

The complete set of material parameters are given in Table 5.

Table 5: Material parameter set II for Aegirite

r	j	α_{rj}	β_{rj}	γ_{rj}	ξ_{rj}
1	1	0.700	0.000	-0.500	1.532
1	2	3.942	0.000	-0.410	1.728
1	3	0.000	0.000	0.000	0.000
2	1	1.000	0.385	-0.500	0.334
2	2	3.685	0.000	-0.500	1.726
2	3	0.000	0.000	0.000	0.000
3	1	0.000	0.000	0.000	0.000
3	2	4.391	0.000	-0.500	2.289
3	3	0.000	4.028	-0.500	1.200

Using this material parameter set II and the metric tensors (3.71) the relative error is 1.62%.

3.4. Transverse Isotropy.

Transverse isotropy is characterized by one preferred direction which is chosen to be the X_3-direction of the underlying cartesian base system. Therefore the free energy (3.1) has to be invariant with respect to all transformations $\boldsymbol{Q}$ of the material symmetry group $\mathcal{G}^{ti}$, given by

$$\boldsymbol{Q}(\alpha, \boldsymbol{e}_3) = \cos(\alpha)\mathbf{1} + \sin(\alpha) \overset{3}{\boldsymbol{e}}\, \boldsymbol{e}_3 + (1 - \cos(\alpha))\boldsymbol{e}_3 \otimes \boldsymbol{e}_3 \,, \tag{3.72}$$

where $\overset{3}{\boldsymbol{e}}$ denotes the third-order permutation tensor. The general form of the anisotropic metric, satisfying (3.3) for all $\boldsymbol{Q} \in \mathcal{G}^{ti}$, is

$$\boldsymbol{G}^{ti} = \mathrm{diag}(a, a, b) \quad \text{with} \quad \mathrm{Cof}\boldsymbol{G}^{ti} = \mathrm{diag}(a\, b, a\, b, a^2)\,. \tag{3.73}$$

In this situation it is useful to compute a functional basis explicitely, based on the evaluation of the characteristic polynomial

$$\begin{aligned} \det[\boldsymbol{C} - \boldsymbol{G}^{ti}] &= \det\boldsymbol{C} - \mathrm{tr}[\mathrm{Adj}[\boldsymbol{C}]\boldsymbol{G}^{ti}] + \mathrm{tr}[\boldsymbol{C}\mathrm{Adj}[\boldsymbol{G}^{ti}]] - \det\boldsymbol{G}^{ti} \\ &= \det\boldsymbol{C} - \mathrm{Cof}\boldsymbol{C} \cdot \boldsymbol{G}^{ti} + \boldsymbol{C} \cdot \mathrm{Cof}\boldsymbol{G}^{ti} - \det\boldsymbol{G}^{ti}\,, \end{aligned} \tag{3.74}$$

see e.g. de Boer & Schröder [12]. The parameters a and b have to be interpreted as additional (positive) material parameters. The evaluation of (3.74) yields, after ordering with respect to the constant coefficients $a, b, ab, a^2, 1$:

$$\mathrm{Cof}C_{11} + \mathrm{Cof}C_{22}\,, \quad \mathrm{Cof}C_{33}\,, \quad C_{11} + C_{22}\,, \quad C_{33}\,, \quad \det\boldsymbol{C}\,. \tag{3.75}$$

All these individual terms of the functional basis are polyconvex, the proofs are given in Schröder & Neff [32, 33]. The generalization coming along with the new concept induces the introduction of the alternative invariant basis

$$I_1 = \mathrm{tr}\boldsymbol{C}\,, \quad I_2 = \mathrm{tr}[\mathrm{Cof}\boldsymbol{C}]\,, \quad I_3 = \det\boldsymbol{C}\,, \quad J_4 = \mathrm{tr}[\boldsymbol{C}\boldsymbol{G}^{ti}]\,, \quad J_5 = \mathrm{tr}[\mathrm{Cof}[\boldsymbol{C}]\boldsymbol{G}^{ti}]\,. \tag{3.76}$$

The proof of polyconvexity of J_4 and J_5 is given in (3.6). The transversely isotropic free energy function is assumed to be of the type

$$\psi^{ti} := \hat{\psi}^{ti}(I_1, I_2, I_3, J_4, J_5)\,. \tag{3.77}$$

The second Piola-Kirchhoff stresses are computed via

$$\begin{aligned} \boldsymbol{S} = 2\frac{\partial\psi^{ti}}{\partial\boldsymbol{C}} = 2 \ & \left[\left(\frac{\partial\psi^{ti}}{\partial I_1} + \frac{\partial\psi^{ti}}{\partial I_2} I_1\right)\mathbf{1} - \frac{\partial\psi^{ti}}{\partial I_2}\boldsymbol{C} + \left(\frac{\partial\psi^{ti}}{\partial I_3} I_3 + \frac{\partial\psi^{ti}}{\partial J_5} J_5\right)\boldsymbol{C}^{-1}\right. \\ & \left. + \frac{\partial\psi^{ti}}{\partial J_4}\boldsymbol{G}^{ti} - \frac{\partial\psi^{ti}}{\partial J_5} I_3 \boldsymbol{C}^{-1}\boldsymbol{G}^{ti}\boldsymbol{C}^{-1}\right]\,. \end{aligned} \tag{3.78}$$

Model Problem I. As a first model problem we consider an additive decomposition of the free energy function as follows

$$\psi^{ti}_I = \psi^{iso}(I_1, I_2, I_3) + \psi^{ti}_1(J_4, J_5)\,, \tag{3.79}$$

where we choose for the isotropic part ψ^{iso} the compressible Mooney-Rivlin model (3.12). For the anisotropic part ψ^{ti}_1 we consider a free energy function in terms of the anisotropic invariants J_4 and J_5, with

$$\psi^{ti}_1 = \frac{1}{\alpha_4(\mathrm{tr}\boldsymbol{G}^{ti})^{\alpha_4}}\eta_1(J_4^{\alpha_4} + J_5^{\alpha_4}), \qquad \forall\ \eta_1 \geq 0,\ \alpha_4 \geq 1\,. \tag{3.80}$$

Evaluating (3.78) yields the second Piola-Kirchhoff stresses in the form

$$\begin{aligned} \boldsymbol{S} \;&= 2\;\; [\{\alpha_1 + \alpha_2 I_1\}\mathbf{1} - \alpha_2 \boldsymbol{C} + \{\delta_1 I_3 - \frac{\delta_2}{2} + \frac{\partial \psi_1^{ti}}{\partial J_5} J_5\}\boldsymbol{C}^{-1} \\ &\qquad + \frac{\partial \psi_1^{ti}}{\partial J_4}\boldsymbol{G}^{ti} - \frac{\partial \psi_1^{ti}}{\partial J_5} I_3 \boldsymbol{C}^{-1}\boldsymbol{G}^{ti}\boldsymbol{C}^{-1})] \,, \end{aligned} \tag{3.81}$$

with the first derivatives of (3.80) with respect to the anisotropic invariants J_4 and J_5

$$\frac{\partial \psi_1^{ti}}{\partial J_4} = \frac{1}{\mathrm{tr}(\boldsymbol{G}^{ti})^{\alpha_4}} \eta_1 J_4^{\alpha_4 - 1} \,, \qquad \frac{\partial \psi_1^{ti}}{\partial J_5} = \frac{1}{\mathrm{tr}(\boldsymbol{G}^{ti})^{\alpha_4}} \eta_1 J_5^{\alpha_4 - 1} \,. \tag{3.82}$$

Let us first enforce the condition of a stress-free reference configuration, $\boldsymbol{S}|_{C=1} = \mathbf{0}$. At the natural state the values of the invariants are

$$I_1 = 3 \,,\; I_2 = 3 \,,\; I_3 = 1 \,,\; J_4 = \mathrm{tr}\boldsymbol{G}^{ti} =: g \,,\; J_5 = \mathrm{tr}\boldsymbol{G}^{ti} =: g \,, \tag{3.83}$$

and the stress tensor appears in the form

$$\boldsymbol{S}|_{C=1} \;= 2\,\{\, \underbrace{\left(\frac{\partial \psi_I^{ti}}{\partial I_1} + 2\frac{\partial \psi_I^{ti}}{\partial I_2} + \frac{\partial \psi_I^{ti}}{\partial I_3} + \frac{\partial \psi_I^{ti}}{\partial J_5} g \right)}_{:=\, x_1^* \,=\, 0} \mathbf{1} + \underbrace{\left(\frac{\partial \psi_I^{ti}}{\partial J_4} - \frac{\partial \psi_I^{ti}}{\partial J_5} \right)}_{:=\, x_2^* \,=\, 0} \boldsymbol{G}^{ti} \} \;. \tag{3.84}$$

In this case the second condition, $x_2^* = 0$, is automatically fulfilled. Thus, only the first condition, $x_1^* = 0$, must be enforced which leads to the following calculation of the dependent material parameter $\delta_2 \in \mathbb{R}^+$

$$\delta_2 = 2\alpha_1 + 4\alpha_2 + 2\delta_1 + 2\eta_1 \,. \tag{3.85}$$

Model Problem II. The second model is given by the following isotropic and anisotropic decomposition

$$\psi_{II}^{ti} := \psi^{iso} + \psi_2^{ti} \,. \tag{3.86}$$

The isotropic part ψ^{iso} given in (3.12) is used. As a second possible anisotropic part of the material model problem we consider

$$\psi_2^{ti} = \eta_1 (J_4^{\alpha_4} + \beta_1 J_5^{\alpha_5}) \,, \qquad \forall\; \eta_1 \,, \beta_1 \geq 0 \,,\; \alpha_4 \,, \alpha_5 \geq 1 \,, \tag{3.87}$$

with the first derivatives with respect to J_4 and J_5

$$\frac{\partial \psi_2^{ti}}{\partial J_4} = \alpha_4 \eta_1 J_4^{\alpha_4 - 1}, \quad \frac{\partial \psi_2^{ti}}{\partial J_5} = \alpha_5 \eta_1 \beta_1 J_5^{\alpha_5 - 1} \,. \tag{3.88}$$

In order to satisfy the condition of a stress-free reference configuration we have to meet both requirements, $x_1^* = 0$ and $x_2^* = 0$, given in (3.84). Here we obtain the following dependencies between the isotropic and anisotropic material parameters

$$\begin{aligned} x_1^* = 0 : &\quad \left.\frac{\partial \psi_{II}^{ti}}{\partial J_4}\right|_{C=1} = \left.\frac{\partial \psi_{II}^{ti}}{\partial J_5}\right|_{C=1} \;\Rightarrow\; \beta_1 = \frac{\alpha_4}{\alpha_5} g^{\alpha_4 - \alpha_5} \,, \\ x_2^* = 0 : &\quad \delta_2 = 2\alpha_1 + 4\alpha_2 + 2\delta_1 + 2\frac{\partial \psi_{II}^{ti}}{\partial J_5} J_5|_{C=1} \\ &\quad \Rightarrow \quad \delta_2 = 2\alpha_1 + 4\alpha_2 + 2\delta_1 + 2\alpha_4 \eta_1 g^{\alpha_4} \,. \end{aligned} \tag{3.89}$$

Homogeneous Biaxial Tension Test. Let us consider a deformation driven homogeneous biaxial compression/tension test. The unit cube is discretized with one eight-noded standard displacement element. The deformed configuration and the boundary conditions are depicted in Figure 8. The specimen is equally stretched in x_1- and x_2-direction, where the biaxial stretches are driven in the range of $\lambda = 0.2$ up to $\lambda = 2.3$; the stretches are defined by $\lambda = (l_1 + u_1)/l_1 = (l_2 + u_2)/l_2$.

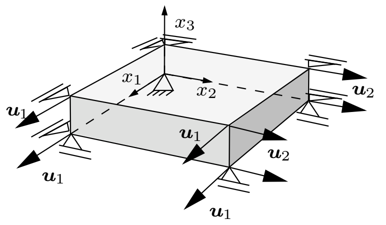

Figure 8: Boundary conditions of the homogeneous biaxial compression/tension test.

The preferred direction of the material is oriented parallel to the x_1-direction. We choose an unimodular metric tensor $\boldsymbol{G}^{ti}$ of the type

$$\boldsymbol{G}^{ti} = \operatorname{diag}\left(\gamma_1^2, \frac{1}{\gamma_1}, \frac{1}{\gamma_1}\right) . \tag{3.90}$$

For the simulation we use the material parameters listed in Table 6. The documented Young's moduli are calculated from the coefficients of the inverse fourth-order elasticity tensor at the reference configuration: $E_1 = 1/\mathbb{C}^{-1}_{1111}$ and $E_2 = 1/\mathbb{C}^{-1}_{2222}$.

Table 6: Table of material parameters (MP) and Young's moduli (YM)

	ψ_I^{ti}		ψ_{II}^{ti}	
MP vs. Case	1	2	1	2
γ_1	2.0	20.0	2.0	5.0
α_1	8.0	8.0	8.0	8.0
α_2	0.0	0.0	0.0	0.0
δ_1	10.0	10.0	10.0	10.0
(δ_2)	56.0	56.0	786.0	9868.24
η_1	10.0	10.0	1.0	0.1
(β_1)	-	-	7.50	38.10
α_4	2.0	2.0	3.0	3.0
α_5	-	-	2.0	2.0
YM				
E_1	115.49	140.20	3367.12	57824.63
$E_2 = E_3$	67.05	56.78	622.86	680.37
E_1/E_2	1.72	2.47	5.41	84.99

$(\cdot)$:= dependent

The first Piola-Kirchhoff stresses in x_1-direction and x_2-direction with respect to the stretch λ can be seen in Figure 9.

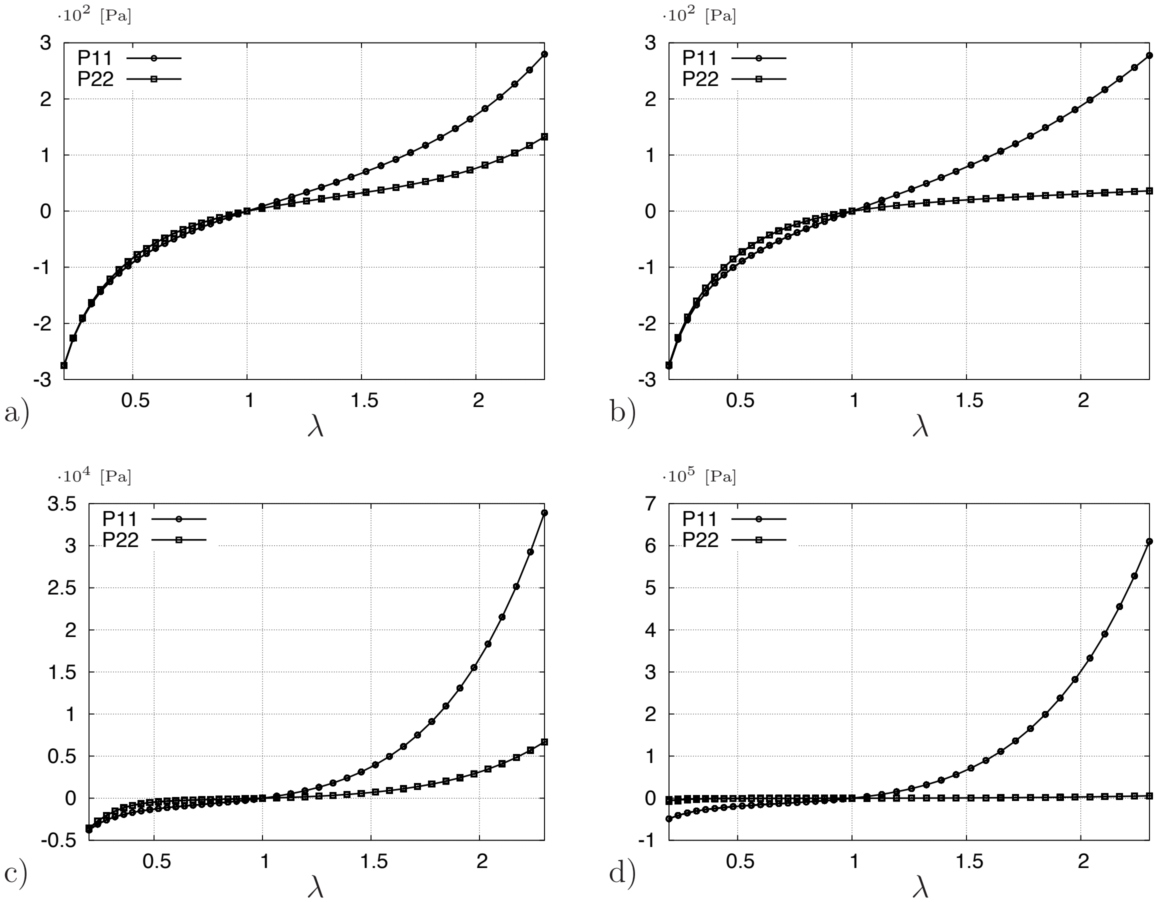

Figure 9: First Piola-Kirchhoff stresses in x_1-direction and x_2-direction versus stretch λ: a) $\psi^{ti}_{I,1}$, b) $\psi^{ti}_{I,2}$, c) $\psi^{ti}_{II,1}$, d) $\psi^{ti}_{II,2}$.

3.5. Orthotropy.

In the orthotropic case we introduce the second-order tensor $\boldsymbol{G}^o$ in such a way that it is invariant with respect to the transformations of the elements $\boldsymbol{Q}$ of the material symmetry group $\mathcal{G}^o$:

$$\mathcal{G}^o = (\boldsymbol{R}_1, \boldsymbol{R}_2, \boldsymbol{R}_3)\ . \tag{3.91}$$

Here $\boldsymbol{R}_1, \boldsymbol{R}_2, \boldsymbol{R}_3$ are reflections with respect to the X_2–X_3–, X_1–X_3– and X_1–X_2-plane defined by the matrices

$$\boldsymbol{R}_1 = \mathrm{diag}(-1,1,1)\,,\ \boldsymbol{R}_2 = (1,-1,1)\,,\ \boldsymbol{R}_3 = \mathrm{diag}(1,1,-1)\,, \tag{3.92}$$

respectively. For the chosen reference frame the general representation is

$$\boldsymbol{G}^o = \mathrm{diag}(a,b,c) \quad \Rightarrow \quad \mathrm{Cof}\boldsymbol{G}^o = \mathrm{diag}(b\ c, a\ c, a\ b)\,. \tag{3.93}$$

The evaluation of (3.74) yields, after substituting $\{\boldsymbol{G}^{ti}, \mathrm{Cof}\boldsymbol{G}^{ti}\}$ for $\{\boldsymbol{G}^o, \mathrm{Cof}\boldsymbol{G}^o\}$ and ordering with respect to the constant coefficients $a, b, c, bc, ac, ab, 1$:

$$\mathrm{Cof}C_{11}\,, \quad \mathrm{Cof}C_{22}\,, \quad \mathrm{Cof}C_{33}\,, \quad C_{11}\,, \quad C_{22}\,, \quad C_{33}\,, \quad \det\boldsymbol{C}\,, \tag{3.94}$$

respectively. Let us remind that the seven terms in (3.94) build the orthotropic functional basis. Furthermore, all these individual terms are polyconvex, the proofs are given in [32, 33].

Model Problem. In the final example we consider an orthotropic free energy function. The potential is governed by the compressible Mooney-Rivlin material (3.12) and the anisotropic metric based terms (3.66). Here we set $n = 3, m = 3$ in (3.66) and take account of the orthotropic metric tensors

$$\boldsymbol{G}_j^o = \begin{bmatrix} a_j & 0 & 0 \\ 0 & b_j & 0 \\ 0 & 0 & c_j \end{bmatrix} \quad \text{with} \quad a_j\,,\ b_j\,,\ c_j > 0\,. \tag{3.95}$$

Let us now approximate the orthotropic material Acenaphthene with the proposed model. The elasticity moduli for the orthotropic material Acenaphthene as well as the characteristic surface of Young's moduli are given in Figure 10, parameters are taken again from Simmons & Wang [38].

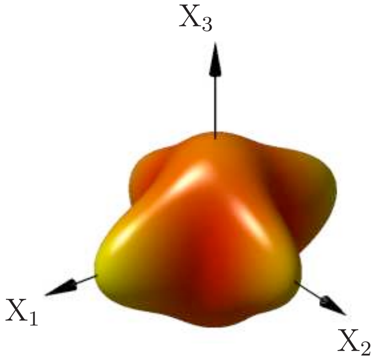

$$\mathbb{C}^{(V)exp} = \begin{bmatrix} 13.8 & 2.1 & 4.1 & 0 & 0 & 0 \\ & 12.6 & 4.6 & 0 & 0 & 0 \\ & & 11.2 & 0 & 0 & 0 \\ & & & 1.9 & 0 & 0 \\ & sym. & & & 2.7 & 0 \\ & & & & & 2.9 \end{bmatrix}.$$

Figure 10: Characteristic surface of Young's moduli and elasticities of Acenaphthene [GPa].

The non-vanishing isotropic material parameters are

$$\delta_1 = 0.0077\,,\ \delta_2 = 0.0154\,, \tag{3.96}$$

and the set of anisotropic material parameters is listed in Table 7. We get three orthotropic metric tensors in the form

$$\begin{aligned} \boldsymbol{G}_1^o &= \operatorname{diag}(0.016, 0.0000002, 0.394)\,, \\ \boldsymbol{G}_2^o &= \operatorname{diag}(0.640, 0.0000001, 0.128)\,, \\ \boldsymbol{G}_3^o &= \operatorname{diag}(0.0000002, 0.716, 0.273)\,, \end{aligned} \tag{3.97}$$

and the fitted orthotropic tangent moduli is finally given by

$$\mathbb{C}^{(V)comp} = \begin{bmatrix} 13.75 & 2.16 & 4.07 & 0 & 0 & 0 \\ & 12.60 & 4.58 & 0 & 0 & 0 \\ & & 11.23 & 0 & 0 & 0 \\ & & & 2.39 & 0 & 0 \\ & sym. & & & 2.63 & 0 \\ & & & & & 2.69 \end{bmatrix}. \tag{3.98}$$

Under consideration of (3.96) and (3.97) we obtain a relative error e of 2.28%.

Table 7: Material parameter set for Acenaphthene

r	j	α_{rj}	β_{rj}	γ_{rj}	ξ_{rj}
1	1	1.037	0.069	-0.134	0.246
1	2	1.918	0.944	-0.260	0.283
1	3	2.242	1.419	-0.479	0.292
2	1	0.379	0.091	-0.286	0.513
2	2	2.173	1.993	-0.383	0.206
2	3	1.815	1.143	0.179	0.034
3	1	1.287	0.583	0.010	0.234
3	2	1.880	1.094	-0.489	0.445
3	3	2.610	1.461	-0.472	0.487

4. Conclusion.

In this paper we have proposed a new method for the construction of anisotropic polyconvex hyperelastic models. The main goal was the introduction of a second-order, symmetric, positive definite structural tensor – motivated by some basic crystallographic geometric relations – incorporating the symmetry properties of the underlying crystal class. The great advantage of the proposed framework is that the deduced generic invariant functions automatically fulfill the polyconvexity condition and satisfy the requirement of a stress-free reference configuration. Proofs of the polyconvexity condition as well as of the coercivity condition have been given in detail. Restrictions coming along with the usage of second-order structural tensors concerning the functional bases of some crystal classes have been pointed out.

Acknowledgement: Financial support from DFG (research grant NE 902/2-1 SCHR 570/6-1) is greatfully acknowledged.

A . Proof of Coercivity.

Let us recall for symmetric, positive definite $\boldsymbol{G}_j$

$$\begin{aligned}
g_j &= \operatorname{tr}\boldsymbol{G}_j = \operatorname{tr}[\boldsymbol{H}_j\boldsymbol{H}_j^T] = \|\boldsymbol{H}_j\|^2 > 0\\
J_{4j} &= \operatorname{tr}[\boldsymbol{C}\,\boldsymbol{G}_j] = \langle \boldsymbol{F}^T\boldsymbol{F}, \boldsymbol{H}_j\boldsymbol{H}_j^T\rangle = \langle \boldsymbol{F}\boldsymbol{H}_j, \boldsymbol{F}\boldsymbol{H}_j\rangle\\
&= \|\boldsymbol{F}\,\boldsymbol{H}_j\|^2 = \|\boldsymbol{H}_j^T\,\boldsymbol{F}^T\|^2 \geq \lambda_{\min}(\boldsymbol{H}_j\boldsymbol{H}_j^T)\|\boldsymbol{F}^T\|^2 = \lambda_{\min}(\boldsymbol{G}_j)\|\boldsymbol{F}\|^2\,,\\
J_{5j} &= \operatorname{tr}[\operatorname{Cof}[\boldsymbol{C}]\,\boldsymbol{G}_j] = \langle \operatorname{Cof}\boldsymbol{F}^T\operatorname{Cof}\boldsymbol{F}, \boldsymbol{H}_j\boldsymbol{H}_j^T\rangle = \langle \operatorname{Cof}[\boldsymbol{F}]\,\boldsymbol{H}_j, \operatorname{Cof}[\boldsymbol{F}]\,\boldsymbol{H}_j\rangle = \|\operatorname{Cof}[\boldsymbol{F}]\,\boldsymbol{H}_j\|^2\\
&= \|\boldsymbol{H}_j^T\operatorname{Cof}\boldsymbol{F}^T\|^2 \geq \lambda_{\min}(\boldsymbol{H}_j\boldsymbol{H}_j^T)\|\operatorname{Cof}\boldsymbol{F}^T\|^2 = \lambda_{\min}(\boldsymbol{G}_j)\|\operatorname{Cof}\boldsymbol{F}\|^2\,,\\
I_3 &= \det\boldsymbol{C} = (\det\boldsymbol{F})^2 \leq \frac{1}{3\sqrt{3}}\|\operatorname{Cof}\boldsymbol{F}\|^3\,,
\end{aligned}\tag{A.1}$$

for the last inequality see Hartmann & Neff [15]. Since $\boldsymbol{G}_j$ is always strictly positive definite we know that the smallest eigenvalue $\lambda_{\min}(\boldsymbol{G}_j) > 0$ is strictly positive.

With these preliminaries let us proceed to show that the anisotropic energy ψ_2^{aniso} satisfies a local coercivity condition, which is needed, together with polyconvexity of ψ_2^{aniso} to ensure the existence of global energy minimizers. Coercivity is a condition that ensures that the energy grows fast enough for large deformation gradients $\boldsymbol{F}$. More precisely by local coercivity we mean an estimate of the type, see Ball [3],

$$\forall\,\boldsymbol{F}\in\mathbb{M}^{3\times3}: \quad \psi_2^{aniso}(\boldsymbol{F}) \geq C_1\,(\|\boldsymbol{F}\|^p + \|\operatorname{Cof}\boldsymbol{F}\|^q) - C_2\,,\quad p\geq 2\,,\ q\geq\frac{3}{2}\,,\tag{A.2}$$

with constants $C_1, C_2 \geq 0$ and $C_1 > 0$.

The function ψ_2^{aniso} has the generic form (taking only the relevant structure into account, i.e. setting $\alpha_{rj}=\alpha$, $\beta_{rj}=\beta$, $\gamma_{rj}=\gamma$, $g_j=g$, $J_{4j}=J_4$, $J_{5j}=J_5$)

$$\psi_2^{aniso}(\boldsymbol{F}) = \frac{1}{1+\alpha}\frac{1}{g^\alpha}J_4^{1+\alpha} + \frac{1}{1+\beta}\frac{1}{g^\beta}J_5^{1+\beta} + \frac{g}{\gamma}\,I_3^{-\gamma}\,.\tag{A.3}$$

Thus it follows easily, taking the relations (A.1) into account, that for $\alpha,\beta\geq 0$

$$\begin{aligned}
\psi_2^{aniso}(\boldsymbol{F}) &\geq \frac{1}{1+\alpha}\frac{1}{g^\alpha}\,J_4 + \frac{1}{1+\beta}\frac{1}{g^\beta}J_5 + \frac{g}{\gamma}\,I_3^{-\gamma}\\
&\geq \frac{1}{1+\alpha}\frac{1}{g^\alpha}\,\lambda_{\min}(\boldsymbol{G}_j)\,\|\boldsymbol{F}\|^2 + \frac{1}{1+\beta}\frac{1}{g^\beta}\,\lambda_{\min}(\boldsymbol{G}_j)\,\|\operatorname{Cof}\boldsymbol{F}\|^2 + \frac{g}{\gamma}\,I_3^{-\gamma}\\
&= c_1^+\,\|\boldsymbol{F}\|^2 + c_2^+\,\|\operatorname{Cof}\boldsymbol{F}\|^2 + \frac{g}{\gamma}\,(\det\boldsymbol{F})^{-2\gamma}\,,
\end{aligned}\tag{A.4}$$

for some given constants c_1^+, $c_2^+ > 0$. In case that γ is positive we have shown (A.2) with $C_1 = \min(c_1^+, c_2^+)$, $C_2 = 0$ and $p = q = 2$.

In the case where γ is negative with $0 \geq \gamma \geq -\frac{1}{2}$ we may continue estimating

$$\begin{aligned}
\psi_2^{aniso}(\boldsymbol{F}) &\geq c_1^+\,\|\boldsymbol{F}\|^2 + c_2^+\,\|\operatorname{Cof}\boldsymbol{F}\|^2 + \frac{g}{\gamma}\,(\det\boldsymbol{F})^{-2\gamma}\,,\\
&\geq c_1^+\,\|\boldsymbol{F}\|^2 + c_2^+\,\|\operatorname{Cof}\boldsymbol{F}\|^2 - c_3^+\,(\det\boldsymbol{F})^{-2\gamma}\,,\\
&= c_1^+\,\|\boldsymbol{F}\|^2 + c_2^+\,\|\operatorname{Cof}\boldsymbol{F}\|^2 - c_3^+\,((\det\boldsymbol{F})^2)^{|\gamma|}\,,
\end{aligned}$$

$$
\begin{aligned}
&\geq c_1^+ \, \|\boldsymbol{F}\|^2 + c_2^+ \, \|\operatorname{Cof}\boldsymbol{F}\|^2 - c_3^+ \, [\det \boldsymbol{F} + 1] \,, \quad 0 \leq |\gamma| \leq \frac{1}{2} \\
&\geq c_1^+ \, \|\boldsymbol{F}\|^2 + c_2^+ \, \|\operatorname{Cof}\boldsymbol{F}\|^2 - c_3^+ \, [\frac{1}{\sqrt{3\sqrt{3}}} \, \|\operatorname{Cof}\boldsymbol{F}\|^{\frac{3}{2}} + 1] \,. \qquad \text{(A.5)}
\end{aligned}
$$

It is obvious that for all $k_1, k_2 > 0$ there exist numbers $\tilde{k}_1, \tilde{k}_2 > 0$ such that

$$
\forall \, x \in \mathbb{R}^+ : \quad k_1 \, x^2 - k_2 \, x^{3/2} \geq \tilde{k}_1 \, x^{3/2} - \tilde{k}_2 \,. \qquad \text{(A.6)}
$$

Applying this reasoning on $x = \|\operatorname{Cof}\boldsymbol{F}\|$ yields the existence of numbers C_2^+, $C_3^+ > 0$ such that

$$
\begin{aligned}
\psi_2^{aniso}(\boldsymbol{F}) &\geq c_1^+ \, \|\boldsymbol{F}\|^2 + c_2^+ \, \|\operatorname{Cof}\boldsymbol{F}\|^2 - c_3^+ \, [\frac{1}{\sqrt{3\sqrt{3}}} \, \|\operatorname{Cof}\boldsymbol{F}\|^{\frac{3}{2}} + 1] \\
&\geq c_1^+ \, \|\boldsymbol{F}\|^2 + C_2^+ \, \|\operatorname{Cof}\boldsymbol{F}\|^{3/2} - C_3^+ \,. \qquad \text{(A.7)}
\end{aligned}
$$

This shows local coercivity with $C_1 = \min(c_1^+, C_2^+)$ and $p = 2$ and $q = \frac{3}{2}$ also for $0 \geq \gamma \geq -\frac{1}{2}$.

References

[1] J. M. Ball. Convexity conditions and existence theorems in non–linear elasticity. *Archive for Rational Mechanics and Analysis*, 63:337–403, 1977.

[2] J.M. Ball. Constitutive inequalities and existence theorems in nonlinear elastostatics. In R.J. Knops, editor, *Herriot Watt Symposion: Nonlinear Analysis and Mechanics.*, volume 1, pages 187–238. Pitman, London, 1977.

[3] J.M. Ball. Some open problems in elasticity. In *Geometry, Mechanics and Dynamics*, pages 3–59. Springer, New York, 2002.

[4] J.M. Ball and R.D. James. Proposed experimental tests of a theory of fine microstructure and the two well problem. *Philosophical Transactions of the Royal Society of London*, 338:389–450, 1992.

[5] D. Balzani. *Polyconvex anisotropic energies and modeling of damage applied to arterial walls.* PhD thesis, 2006.

[6] D. Balzani, P. Neff, J. Schröder, and G.A. Holzapfel. A polyconvex framework for soft biological tissues. Adjustment to experimental data. *International Journal of Solids and Structures*, 43(20):6052–6070, 2006.

[7] J.P. Boehler. Lois de comportement anisotrope des milieux continus. *Journal de Mécanique*, 17(2):153–190, 1978.

[8] J.P. Boehler. A simple derivation of representations for non-polynomial constitutive equations in some cases of anisotropy. *Zeitschrift für angewandte Mathematik und Mechanik*, 17:157–167, 1979.

[9] J.P. Boehler. Introduction to the invariant formulation of anisotropic constitutive equations. In J.P. Boehler, editor, *Applications of Tensor Functions in Solid Mechanics*, CISM Course No. 292. Springer, 1987.

[10] P.G. Ciarlet. *Three-Dimensional Elasticity.*, volume 1 of *Studies in Mathematics and its Applications.* Elsevier, Amsterdam, first edition, 1988.

[11] B. Dacorogna. *Direct Methods in the Calculus of Variations.*, volume 78 of *Applied Mathematical Sciences.* Springer, Berlin, first edition, 1989.

[12] R. de Boer and J. Schröder. *Tensor Calculus for Engineers with Applications to Continuum and Computational Mechanics.* Springer, to appear in 2008.

[13] Y.I. Dimitrienko. *Tensor Analysis and Nonlinear Tensorfunctions.* Kluwer Academic Publishers, 2002.

[14] P.R. Halmos. *Finite-dimensional Vector Spaces.* Van Nostrand, New York, 1958.

[15] S. Hartmann and P. Neff. Polyconvexity of generalized polynomial type hyperelastic strain energy functions for near incompressibility. *International Journal of Solids and Structures*, 40:2767–2791, 2003.

[16] M. Itskov and N. Aksel. A class of orthotropic and transversely isotropic hyperelastic constitutive models based on a polyconvex strain energy function. *International Journal of Solids and Structures*, 41:3833–3848, 2004.

[17] N. Kambouchev, J. Fernandez, and R. Radovitzky. A polyconvex model for materials with cubic symmetry. *Modelling and Simulation in Material Science and Engineering*, 15:451–467, 2007.

[18] A. Krawietz. *Materialtheorie - Mathematische Beschreibung des phänomenologischen thermomechanischen Verhaltens.* Springer, 1986.

[19] I.S. Liu. On representations of anisotropic invariants. *International Journal of Engineering Science*, 20:1099–1109, 1982.

[20] A.E.H. Love. *Lehrbuch der Elastizität.* B.G. Teubner Sammlung von Lehrbüchern: Mathematische Wissenschaften Band XXIV. 1907.

[21] B. Markert, W. Ehlers, and N. Karajan. A general polyconvex strain-energy function for fiber-reinforced materials. *Proceedings in Applied Mathematics and Mechanics*, 5:245–246, 2005.

[22] J.E. Marsden and J.R. Hughes. *Mathematical Foundations of Elasticity.* Prentice-Hall, 1983.

[23] A. Menzel and P. Steinmann. On the comparison of two strategies to formulate orthotropic hyperelasticity. *Journal of Elasticity*, 62:171–201, 2001.

[24] J. Merodio and P. Neff. A note on tensile instabilities and loss of ellipticity for a fiber-reinforced nonlinearly elastic solid. *Archives of Mechanics*, 58:293–303, 2006.

[25] J. Merodio and R.W. Ogden. Instabilities and loss of ellipticity in fiber-reinforced compressible non-linearly elastic solids under plane deformation. *International Journal of Solids and Structures*, 40:4707–4727, 2003.

[26] A. Mielke. Necessary and sufficient conditions for polyconvexity of isotropic functions. *Journal of Convex Analysis*, 12:291–314, 2005.

[27] C.B. Morrey. Quasi–convexity and the lower semicontinuity of multiple integrals. *Pacific Journal of Mathematics*, 2:25–53, 1952.

[28] S. Müller. Variational models for microstructure and phase transitions. In *Calculus of Variations and Geometric Evolutions Problems*, Lecture Notes in Math. 1713, pages 85–210. Springer, Berlin, 1999.

[29] F.E. Neumann. *Vorlesungen über die Theorie der Elastizität der festen Körper and des Lichtäthers.* Teubner, 1885.

[30] I. Rechenberg. *Evolutionsstrategie '94.* Frommann-Holzboog, 1994.

[31] J. Rychlewski and J.M. Zhang. On representations of tensor functions: a review. *Advances in Mechanics*, 14:75–94, 1991.

[32] J. Schröder and P. Neff. On the construction of polyconvex anisotropic free energy functions. In C. Miehe, editor, *Proceedings of the IUTAM Symposium on Computational Mechanics of Solid Materials at Large Strains*, pages 171–180. Kluwer Academic Publishers, 2001.

[33] J. Schröder and P. Neff. Invariant formulation of hyperelastic transverse isotropy based on polyconvex free energy functions. *International Journal of Solids and Structures*, 40:401–445, 2003.

[34] J. Schröder, P. Neff, and D. Balzani. A variational approach for materially stable anisotropic hyperelasticity. *International Journal of Solids and Structures*, 42(15):4352–4371, 2005.

[35] H.P. Schwefel. *Evolution and Optimum Seeking.* Wiley, 1996.

[36] L.A. Shuvalov. *Modern Crystallography IV, Physical Properties of Crystals.* Springer, 1988.

[37] M. Silhavý. *The Mechanics and Thermodynamics of Continuous Media.* Springer, 1997.

[38] G. Simmons and H. Wang. *Single Crystal Elastic Constants and Calculated Aggregate Properties.* The M.I.T. Press, 1971.

[39] G.F. Smith and R.S. Rivlin. Stress-deformation relations for anisotropic solids. *Archive for Rational Mechanics and Analysis*, 1:107–112, 1957.

[40] G.F. Smith and R.S. Rivlin. The strain-energy function for anisotropic elastic materials. *Transactions of the American Mathematical Society*, 88:175–193, 1958.

[41] G.F. Smith, M.M. Smith, and R.S. Rivlin. Integrity bases for a symmetric tensor and a vector. the crystal classes. *Archive for Rational Mechanics and Analysis*, 12:93–133, 1963.

[42] A.J.M. Spencer. Theory of invariants. In A.C. Eringen, editor, *Continuum Physics*, volume 1, pages 239–353. Academic Press, 1971.

[43] D.J. Steigmann. Frame-invariant polyconvex strain-energy functions for some anisotropic solids. *Mathematics and Mechanics of Solids*, 8:497–506, 2003.

[44] E.S. Şuhubi. Thermoelastic solids. In A.C. Eringen, editor, *Continuum Physics*, volume 2. Academic Press, 1975.

[45] H. Xiao. On isotropic extension of anisotropic tensor functions. *Zeitschrift für angewandte Mathematik und Mechanik*, 76(4):205–214, 1996.

[46] J.M. Zhang and J. Rychlewski. Structural tensors for anisotropic solids. *Archives of Mechanics*, 42:267–277, 1990.

[47] Q.-S. Zheng. Theory of representations for tensor functions – a unified invariant approach to constitutive equations. *Applied Mechanics Reviews*, 47:545–587, 1994.

[48] Q.-S. Zheng and A.J.M. Spencer. Tensors which characterize anisotropies. *International Journal of Engineering Science*, 31(5):679–693, 1993.